3-2021

Hazard Mapping for Infrastructure Planning in the Arctic

Christopher I. Amaddio

HAZARD MAPPING FOR INSTRASTRUCTURE PLANNING IN THE ARCTIC

THESIS

Christopher I. Amaddio, 1st Lt, USAF

AFIT-ENV-MS-21-M-201

DEPARTMENT OF THE AIR FORCE
AIR UNIVERSITY

AIR FORCE INSTITUTE OF TECHNOLOGY

Wright-Patterson Air Force Base, Ohio

HAZARD MAPPING FOR INFRASTRUCTURE PLANNING IN THE ARCTIC

THESIS

Presented to the Faculty

Department of Engineering Management

Graduate School of Engineering and Management

Air Force Institute of Technology

Air University

Air Education and Training Command

In Partial Fulfillment of the Requirements for the

Degree of Master of Science in Engineering Management

Christopher I. Amaddio, BS

1st Lt, USAF

February 2021

AFIT-ENV-MS-21-M-201

HAZARD MAPPING FOR INFRASTRUCTURE PLANNING IN THE ARCTIC

Christopher I. Amaddio, BS
1st Lt, USAF

Committee Membership:

Alfred E. Thal, Jr., PhD

Chair

Lt Col Ryan Howell, PhD

Member

Christopher Chini, PhD

Member

Abstract

The Arctic is in the midst of drastic change from the perspective of climate science, economics, and politics. With billions of dollars in Arctic infrastructure and critical missions ongoing, the United States Department of Defense has a serious interest in the stability of the region, as outlined in the 2020 Arctic Strategy. Without the necessary infrastructure planning to mitigate risks from the hazards in the Arctic that are exacerbated by climate change, success will be short lived. This research identified Arctic hazards related to building foundation health using remote sensing data to provide a tool for communicating risk, prioritizing maintenance, and planning future infrastructure projects. Using modern high-resolution aerial photographs, LiDAR, historical aerial photographs, and facility data, a hazard mapping effort identified risks to infrastructure at Thule Air Base, Greenland, based on visible terrain features, surface hydrology, and slope; the distribution of these risks were then compared to existing foundation damage. The analysis indicated abundant and widespread geotechnical hazards at Thule Air Base and a weak relationship to existing foundation damage that requires more research to understand. The resulting hazard maps provide a critical tool for risk assessment and planning as well as a model for other locations to follow.

Acknowledgments

To my family for their endless support. To my mentors, new and old, for their inspiration. Thank you

Christopher I. Amaddio

Table of Contents

Table of Figures

Page

Table of Tables

Page

HAZARD MAPPING FOR INFRASTRUCTURE PLANNING IN THE ARCTIC

Chapter I. Introduction

Built infrastructure, including facilities, transportation networks, and utilities, support the health, safety, and prosperity of organizations and communities around the world. Aging systems and increased human, economic, and environmental pressures threaten these support systems and drive a new focus on building and maintaining resilient infrastructure systems (World Economic Forum, 2019). Climate change is perhaps one of the most significant threats to the resilience of infrastructure systems. Although the characteristics of a resilient system may vary across context and are subject to debate, Seager et al. (2017) list the characteristics of a resilient system as rebound, robustness, extensibility, and adaptation. However, a full picture of these characteristics is incomplete without the identification of the specific hazards that threaten the system. Climate change is a complicated and evolving threat, but it manifests in specific ways that can be defined and identified to improve infrastructure planning and maintenance. A specific region that faces extreme hazards and drastic change compared to the rest of the world is the Arctic, prompting the attention of engineers and planners to work to mitigate the threats to infrastructure.

Change in the Arctic is a commonplace topic for headlines and focuses on political conflict, untapped petroleum reserves, and military exercises (Kapla et al., 2013; Howard, 2009; Shea, 2019). Often ignored are increased engineering challenges and the stress on aging and modern infrastructure that ultimately threaten the health and safety of organizations and communities in the Arctic. Climate change in the Arctic has been characterized by disproportionately increasing air and water temperatures leading to a loss of ice throughout the

landscape (IPCC, 2019). Ice is the foundation of the Arctic ecosystem and human activity in the region. The rising temperature and loss of ice across the Arctic brings economic opportunity for some but creates engineering hazards for its current and future inhabitants. Integrating community goals, existing infrastructure, and future development is critical to adapting to changes (Benkert et al., 2016; Hjort et al., 2018; Seager et al., 2017). The first step of this process is the identification of threats to these goals.

Background

The health of infrastructure in the Arctic is threatened by climate change (IPCC, 2019). The Arctic's reliance on thermal balance makes the threat of a warming climate more acute. Coastal erosion, flooding, earth movement, and permafrost degradation are just some of the major hazards faced in the region (Northern Climate ExChange, 2016). These hazards have been identified across the Arctic circle by many communities and organizations. The United States (U.S.) military, specifically, has operated in the Arctic environment for almost a century; it has made great strides in understanding the environment and has brought a renewed focus to protecting infrastructure across the region in the face of these changes. With the inception of the United States Space Force, and the development of increasing contested missions in the Arctic and Space, investment in the understanding of modern threats is recommended. The northernmost military base, Thule Air Base in northwest Greenland, has faced the challenge of building on permafrost since its construction in 1951. While many investigations and the advancement of Arctic construction have improved the performance of base infrastructure, the spatial distribution of hazards across the base is generally unknown. Therefore, creating a

framework to identify, model, and visualize hazards across the base will increase the viability of existing and future infrastructure.

Climate Change in the Arctic

The Intergovernmental Panel on Climate Change suggests that the average surface temperatures in the Arctic have risen two times faster than the global average. These changes in temperature, along with a decrease in sea ice, increased precipitation, and loss of snow cover, influence each other and act as drivers for climate change around the world (IPCC, 2019). Models suggest that mean near-surface winter air temperatures may rise between 1.5 and 10 degrees Celsius by 2080 (AMAP, 2017). As a result of rising temperatures and a loss of sea ice, precipitation is also projected to increase (Zhang et al., 2012; Kopec et al., 2016; Bintanja et al., 2017). These changes pose a significant threat to the stability of permafrost. Warming air temperatures lead to changes in the temperature and distribution of permafrost, depth of the active layer, and physical state of ground ice (Obu et al., 2019; Romanovsky et al., 2010; Smith and Riseborough, 2002). As these changes progress, it is essential to continue to identify and study the hazards they influence.

Hazard Mapping

Hazard maps are spatial representations of physical processes and conditions that could cause damage (Cova, 1999; Tarolli and Cavalli, 2013). The criteria for a hazard map are ultimately determined by the creator, the user, and the nature of the site (Benkert et al., 2016). Hazard mapping has been completed for much of the northern hemisphere with degrading permafrost as the focus (Daanen et al., 2011; Flynn et al., 2019; Hjort et al., 2018; Karjalainen et

al., 2019; Streletskiy et al., 2012). Researchers have completed large scale analyses of the northern hemisphere and produced maps ranging in extent from the entire northern hemisphere to specific regions or countries. These efforts have relied primarily on ground temperatures, air temperature, active layer thickness, and climate change models to assess the risk of permafrost thaw (Streletskiy et al., 2012). Although these are useful for planning on a large scale, they do not offer the level of detail needed for community level decision-making. More detailed maps are needed for risk assessment at this level. Maps like those created by Benkert et al. (2016) are needed to produce actionable results. Comprehensive, community-focused hazard maps will lead to better long-term planning decisions and ultimately successful adaptation to climate change.

Identifying Permafrost

Permafrost is earth, including soil and bedrock, that exists at 0°C (32°F) or below for at least two consecutive years (Muller, 1947). Covering 23.9% of land in the northern hemisphere (Zhang et al., 2008), the distribution of permafrost is shown in Figure 1. Permafrost is a thermal regime but manifests itself in physical ways that can be viewed in the natural landscape. These visible features are important indications of underlying hazards. Permafrost has traditionally been identified using aerial imagery and field investigations (Hopkins and Karlstrom, n.d.). Modern technologies have been developed to more accurately map ice distribution, but field studies and aerial photography remain a vital component of understanding the landscape (Black, 1976). Although photogrammetry, the process of interpreting photographic information to obtain information about ground objects, is limited in power, it can be used in conjunction with physical samples and field observations to provide a perspective not available from the surface.

Specific features used to identify underlying ice in permafrost include patterned ground, palsas, pingos, thermokarst, and more (Black, 1976; Corte, 1962; Schmertmann et al., 1965). These features are an important piece of mapping the hazards in permafrost regions, and the United States Geological Survey has produced material documenting the identification of these features (Benninghoff, 1953; Boike and Yoshikawa, 2003; Black, 1976; Schmertmann and Taylor, 1965; Corte, 1962).

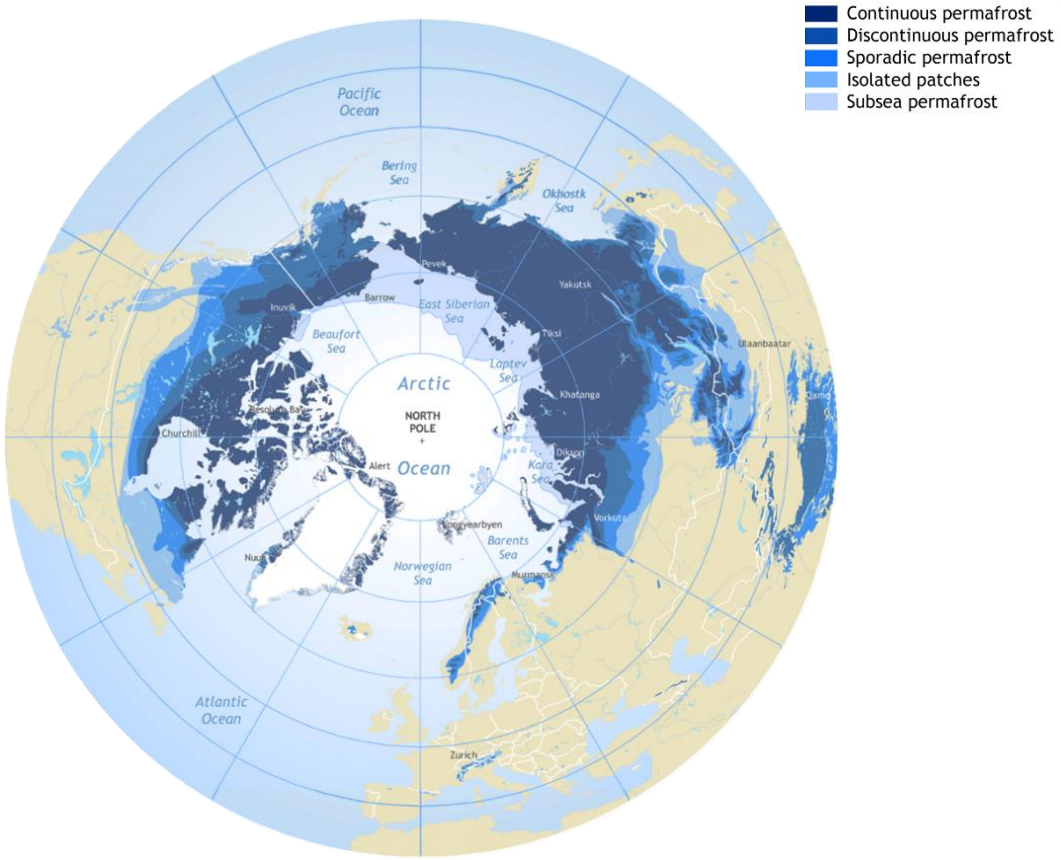

Figure 1. Permafrost in the Northern Hemisphere (International Permafrost Association, 1997)

Historical Perspective

Understanding the hazards facing infrastructure in the Arctic, and specifically Thule Air Base, requires an understanding of the sensitive nature of Arctic terrain and the context of challenges faced in the past. Historical reports of infrastructure challenges during construction and in the years following are critical to informing a complete picture of hazards faced today and provide support for observations made from remote sensing data. Additionally, the fragile state of permafrost leaves it vulnerable to thaw from human disturbances, thus erasing the visible markers of permafrost hazards (Muller, 1947). Activities like the heavy earthwork required for the construction of facilities and pavements involved in the creation of a military installation are extremely transformative for the Arctic landscape. With many of the visible markers of hazards destroyed by these activities, historical aerial photography is a crucial element in mapping the hazards at any location. The nature of climate change in the Arctic also warrants the use of historical photos to help understand the changes to the terrain over time. The utility of a historical perspective is demonstrated in Figure 2, which shows modern facilities placed on areas with observable hazardous terrain. With the accounts of planning (Hunt, 1946; Pick, 1953), construction (Dod, n.d.), and subsequent challenges at Thule Air Base (AFCEL, 1955; McAnerney, 1968; Tobiasson & Lowrey, 1970; Hansen, 1994), combined with historical aerial photography, a more complete understanding of hazards and the potential risks they pose to infrastructure is generated.

Figure 2. Juxtaposition of aerial photos from 1952 and 2018 (citation)

Thule Air Base

Thule Air Base is located on the coast of Baffin Bay in the northwest corner of Greenland. Extreme temperatures, hurricane force winds, and extended periods of total dark and total light pose unique challenges for engineers. The mission of the base is to provide missile warning, space surveillance, and space control to the North American Aerospace Defense Command and United States Space Force; as such, its location is tied directly to these capabilities. Construction began in 1951 as part of a secret Cold War initiative to secure strategic ground between Washington D.C. and Moscow (Dod, n.d.). Originally intended to watch for Soviet activity and launch offensive strikes, it is now part of a constellation of Arctic bases providing missile watch for the U.S. and allied nations. Figure 3 highlights the military activities across the Arctic. With billions of dollars in infrastructure, including critical radar

equipment exceeding 100 million dollars, investment in the understanding of threats to permafrost is warranted. Thule's infrastructure has faced geotechnical challenges, and damage has been observed since its inception (Bjella, 2010; Bjella, 2018). Recorded damages have included the settlement of hangar floors on the order of meters, cracked foundations, and numerous challenges with settlement of the runway (Tobiasson & Lowrey, 1970; Bjella, 2010). Severe damage to the runway shoulder was recorded in August 2020 after a 4-day rain event and raised questions of a possible link to ice under the runway. Events such as this underscore the value of mapping the hydrologic and permafrost related hazards at Thule. Anticipating maintenance challenges and planning future construction sites is an important part of adapting to the changing environment. Understanding the distribution of hazards across the base is a vital part of the goal of a resilient system of infrastructure.

Problem to be Investigated

The health of infrastructure at Thule Air Base is threatened by the changes being experienced in the Arctic. The base sits on top of permafrost extending up to 300 meters deep; with varying permafrost active layer thickness, the risk to infrastructure is abundant but difficult to classify (Bjella, 2018). Since construction in 1951, many facilities have experienced damage ranging from cracked drywall to meters of settlement. Advancement in the understanding of permafrost construction has improved the performance of foundations and other infrastructure, but many other structures are still plagued by inherited flaws, maintenance issues, and climate conditions exceeding design limits. The problem is that although many investigations have been completed for specific facilities across the base, the general distribution of permafrost features, and hydrologic hazards appears generally undocumented.

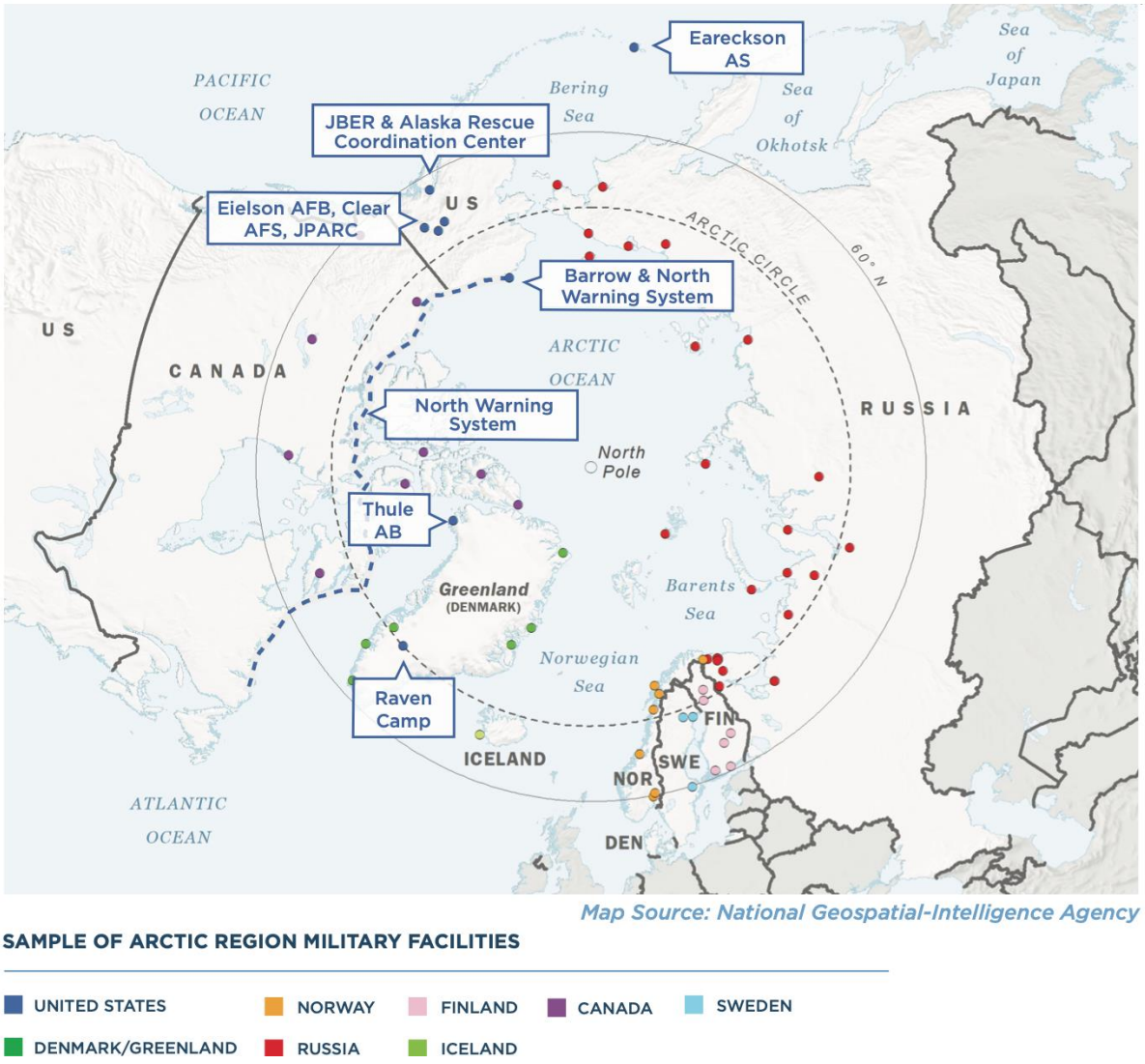

Figure 3. Military Facilities across the Arctic (DoD, 2020)

Research Questions

A spatial visualization of hazards can provide a planning tool to aid in the maintenance of facilities and the placement of future infrastructure. Therefore, the goal of this research is to validate the threats to infrastructure across Thule Air Base by completing a preliminary investigation of the distribution of permafrost and drainage issues across the base. Specifically, the following questions are framed in order to validate and identify the threat of climate change

to the base. These questions aim to build an understanding of the threats to infrastructure and develop a model to assist decision-makers in developing plans for the base.

1. What are the climate trends for Thule Air Base over the past 70 years?
2. What are the permafrost and hydrologic hazards at Thule and what is their spatial distribution?
3. What is the link between hazards and facility damage?

Methodology

The methodology of this research is broken into four major efforts: the analysis of historical weather data, the identification of hazards, a quantification of foundation damage, and exploration of the relationship between foundation damage and hazard. To validate the underlying assumption that Thule Air Base is experiencing warming temperatures and increased rainfall, simple linear regression is completed using available weather data and compared to regional climate projections. Using aerial photography of the base, a preliminary survey of visible permafrost features follows. Hydrologic hazards and ground slope are identified using ESRI's ArcMap and available remote sensing data. Permafrost features, ground slope, and hydrology hazards are mapped separately in ArcMap and then combined to create a cumulative hazard map. The foundation conditions of facilities across the base are then determined using existing investigation reports, inspections, and facility maintenance data. Finally, the cumulative hazard map is compared to recorded facility damage to explore the relationship between permafrost related hazards and infrastructure deterioration.

Significance

Infrastructure in the Arctic is vulnerable to the unique environment and changing climate conditions (Shur et al., 2009; IPCC, 2019; AMAP, 2017; Daanen et al., 2011; Steletskiy et al, 2012). The Arctic is a strategic priority for the U.S. Department of Defense, and the dynamic changes of the environment are a threat garnering increased interest from decision-makers. The Secretary of the Air Force, Barbara Barrett, says "the Arctic is among the world most strategically significant regions – the keystone from which the U.S. Air and Space Forces exercise vigilance" (DoD, 2020). In the 2020 Arctic Strategy, a focus on infrastructure adaptation and security is highlighted as paramount to maintaining critical operations, but the strategy lacks specific steps to achieve these goals. With a constellation of critical bases across the Arctic and evidence of rapid environmental change, the need for a continual focus on hazard identification is evident. This research aims to provide a model for sites to create planning tools to adapt to the challenges today and in the future.

Roadmap

In the development of this research, Chapter II explores the relevant literature related to climate change in the Arctic. This includes reviewing weather data trends, hazard maps, permafrost and hydrologic hazards, the history of Thule Air Base, and finally the technical requirements and costs associated with completing a hazard map. Chapter III details the collection and analysis of weather data, photos, Light Detection and Ranging (LiDAR) data, and facility assessments. Weather data will be used to identify trends across the past 70 years. Remote sensing data will be used to identify and visualize the hazards across the base and test a correlation between facility damage and hazards. The results of the linear regression,

preliminary hazard map, feasibility analysis, and discussion of limitations follow in Chapter IV. The conclusions and recommendations, along with the implications of the findings, are presented in Chapter V.

Chapter II. Literature Review

This chapter discusses climate change in the Arctic, the hazards to infrastructure in the Arctic, the ways to identify and communicate hazards, and the history and infrastructure issues at Thule Air Base in Greenland. The conversation is focused on validating the need to improve the understanding of the relationship between permafrost and infrastructure performance around the Arctic and specifically Thule Air Base.

Climate Change and the Cryosphere

The cryosphere is a term used to refer to all frozen water on earth to include snow, ice, and permafrost (IPCC, 2019; Arenson et al., 2015). With 10% of the land area on earth covered by ice and glaciers, the cryosphere is directly connected to the global climate system through the exchange of water, carbon, and energy (IPCC, 2019). Climate change, driven by increasing concentrations of greenhouse gasses in the atmosphere, has led to a warming of the Arctic at a more substantial rate than the global average (Ballinger et al., 2020). Assuming no change in the current rate of greenhouse gas emissions, the Arctic could warm 4-5°C by 2050; the resulting physical effects would include a total loss of summer sea ice by 2030, a 35% reduction in permafrost, and a 1-2% increase in precipitation per year (IPCC, 2019; AMAP, 2017). Regardless of climate projections, the Arctic is currently experiencing the highest temperatures and lowest sea ice mass since records began in 1900 (AMAP, 2019). These conditions and predictions present a clear risk to the four million inhabitants of the Arctic region (IPCC, 2019). These predictions help inform global conversations, but they do not provide the level of detail needed to assess the risk to individual communities or stakeholders.

Historical weather data helps build models that predict the signals of climate change around the world. Some models focus on characterizing the general trends across the globe or for specific regions to understand anthropogenic influences on climate, inform political decisions, and analyze risk to people across large areas of study (Bindoff et al., 2013; Hartmann et al., 2013; Melillo et al., 2014). Bindoff et al. (2013) synthesized regional climate models that used surface weather data and satellite data to assess the global climate system for anthropogenic influences. They concluded that the spatial availability of weather data did not have a significant influence on the outcome, but they limit their findings to broad statements. Stendel et al. (2008) analyzed climate signals at a 25km resolution for Greenland using an Atmosphere-Ocean General Circulation model and were able to identify more nuanced changes by region. While the resolution of the simulation allows for more precise findings, the reliance on the Arctic model constrains their use to the national level. Lai and Dzombak (2019) used historical weather observations to assess the trends for small regions of the United States in order to inform construction practice. Rather than focus on the coupling of a global or regional model to historical data, their study focused on the statistical analysis of data from local weather stations only. Using Ordinary Least Squares (OLS) regression and a 10-year moving average, they created profiles for small areas across the United States to inform regional decision-making.

While natural variability in climate can mask the local signals of climate change, statistical methods like OLS regression can help more accurately portray the trends at a smaller scale (Martel et al., 2018). The inclusion of the 10-year moving average helps identify trends when yearly or decade-long trends may mask the overall baseline (Karl et al., 1995). While more advanced statistical methods such as wavelet and empirical mode transformation have been used to address the issues with climate data (Lau & Weng, 1995; Carmona & Poveda, 2014),

simple linear regression can yield adequate results in the analysis of climate trends (Franzke, 2012). In OLS regression, a line of best fit is created that minimizes the square of the distance between the predicted and the actual values, thereby allowing for a simple analysis of results when assumptions are met. While these methods have been applied to the United States, published results are not available for remote U.S. assets like those in the Arctic. The inclusion of climate trends is an import part of understanding the hazards in a region, especially one as extreme as the Arctic (Northern Climate ExChange, 2016). While studies like Bjella (2018) have provided suggestions that Thule Air Base is experiencing warming and increasing precipitation trends based on the visual interpretation of the historical data, a more rigorous statistical analysis is needed to validate that a risk of higher temperatures and greater summer precipitation exists for Thule.

Hazards to Arctic Infrastructure

The Arctic is a challenging environment in which to live and to build the infrastructure that supports life. The challenges associated with infrastructure design in Arctic conditions include seasonal freeze and thaw that lead to frost heaving, difficulty in surveying heterogeneous properties of soil with the addition of ice, possible excess water from impervious shallow ground, ice uplift, and extreme thermal stresses (Linell et al., 1980). These challenges are a result of the hazards created by the existence of permafrost. The major hazards of interest in this study are the thawing of permafrost and the experience of frost action from excess surface water. For the purposes of this research, a hazard refers to a natural process or feature that has the potential to cause physical damage to the environment, infrastructure, or people (Agard and Schipper, 2014). While not unique to the Arctic landscape, terrain slope also contributes to the

hazards experienced in the Arctic through its relationship to cryogenic processes and the downslope movement of material, as well as general slope stability considered in geotechnical and foundation engineering. Slope stability is a complex topic in geotechnical engineering, but in general a steeper slope has a greater chance of slope failure (Coduto et al., 2016) and a greater chance of solifluction (Davis, 2001).

Permafrost

Permafrost is earth, existing below freezing continually for two years or greater, regardless of its constituents. Also called permanently frozen soil, it ranges from bedrock to surface deposits and can differ substantially in particle size, water content, and ice features. Permafrost is distinguished from seasonally frozen ground, which is frozen for less than two years continually (Muller, 1947). Covering 23.9% of land in the northern hemisphere, permafrost is a common feature of the Arctic landscape (Zhang et al., 2008). Permafrost is first classified as dry or wet, with dry permafrost or dry frost having little to no water and wet having a mixture of frozen cemented ice and pore water. Dry permafrost exhibits similar characteristics to unfrozen soil from an engineering perspective (Stearns, 1966) and is generally not a hazard to infrastructure. Another distinct feature of permafrost terrain is the active layer. This layer rests above the permanently frozen ground, is delineated by the permafrost table below, and experiences the yearly freeze-thaw cycle (Muller, 1947). The depth of the active layer is influenced by many factors, including air and ground temperatures, vegetation, snow cover, solar radiation, and human activity (Davis, 2001; Muller, 1947; Stearns, 1966). Annual freezing of the active layer can result in heaving of the surface (Andersland & Ladanyi, 2013), and reoccurring frost action contributes to the formation of visible terrain features (Brown et al., 1981).

The unique physical and thermal properties of permafrost influence the hazards associated with it (Arenson et al., 2015), and permafrost varies significantly in structure and density based on the soil particles and ice content (Andersland & Ladanyi, 2004). Permafrost is often categorized by its volumetric ice content with three major categories. Ice-poor soils have less than 50 percent ice in which the ice is generally located in the space between soil particles, whereas ice-rich soils have between 50 and 80 percent ice by volume and dirty ice has greater than 80 percent ice by volume. When the ice content is larger than the porosity of the unfrozen soil, it is called excess ice. These classifications help describe permafrost and additionally aid in the determination of the strength of the soil. Soils with high ice content present a greater risk to infrastructure (Karjalainen et al., 2019; Stearns, 1966). These ice-rich soils are also termed thaw-unstable as they lose much of their bearing capacity when thawed (Muller, 1947). This loss of bearing capacity, which leads to settlement, is the main hazard created by permafrost. These characteristics, however, are simplifications of complex processes; predicting the exact mechanical behavior of frozen soils is based on the interaction of many of these factors and requires continued research (Arenson, 2007).

Features of the Permafrost Landscape

The periglacial environment has many unique features resulting from a combination of extreme temperatures, water, and fine grain soils. The formation of ice below the surface, and the sometimes-visible surface patterns they create, become identifiable from field studies and aerial photos. There are many names for different ice formations, but Davis (2001) lists the major categories as pore ice, segregation ice, ice-wedge ice, pingo ice, and buried ice. Pore ice is frozen water that exists in the pore space between soil particles. This form of ice contributes to a

large part of the first few meters of permafrost and most of the ice below 10 meters. Segregation ice forms through a process of cryosuction, which represents the movement of water through the soil pores upwards towards the lower surface temperatures that creates large layers of ice perpendicular to the temperature gradients. The variable nature of soil water content makes pore ice and segregated ice sporadic and more difficult to identify from surface features. Ice-wedges are formed from the infiltration of water though vertical surface cracks formed by seasonal thermal contraction. As water enters the crack and freezes each season, large, foliated wedges form as seen in Figure 4. In homogenous soils, cracks will form nonorthogonal (hexagonal) shapes similar to those seen in Figure 5 because this shape releases the most strain energy, whereas heterogeneous soils form orthogonal (right-angle) patterns. Ice-wedges can also be identified as active and inactive by the elevation of the center of the shape. Warmer temperatures or other factors halting the growth of wedges melt the top layer of soil causing a depression around the ice, or a high-center polygon, whereas thermal expansion of active wedges in the summer raises the exterior soil creating a low-center polygon. Pingo ice forms when water under hydrostatic pressure lifts the earth and creates a mass of ice underneath. The resulting landforms, called pingos, can be as large as 50 meters tall, while a similar but smaller ice mass landform is called a palsa. Finally, buried ice can result from a number of processes such as recrystallization of snow or deposition from lakes. An important form of buried ice is relict ice, which is defined by Muller (1947) as a remnant of glacial retreat resulting from large ice masses fracturing from a glacier and being randomly deposited; the random nature of this ice and no visible surface features makes this a threat to infrastructure (Bjella, 2015). Features resulting from frost action and the processes of permafrost formation and thaw are numerous and often

named differently across disciplines or research, thereby making it a difficult topic to discuss without context.

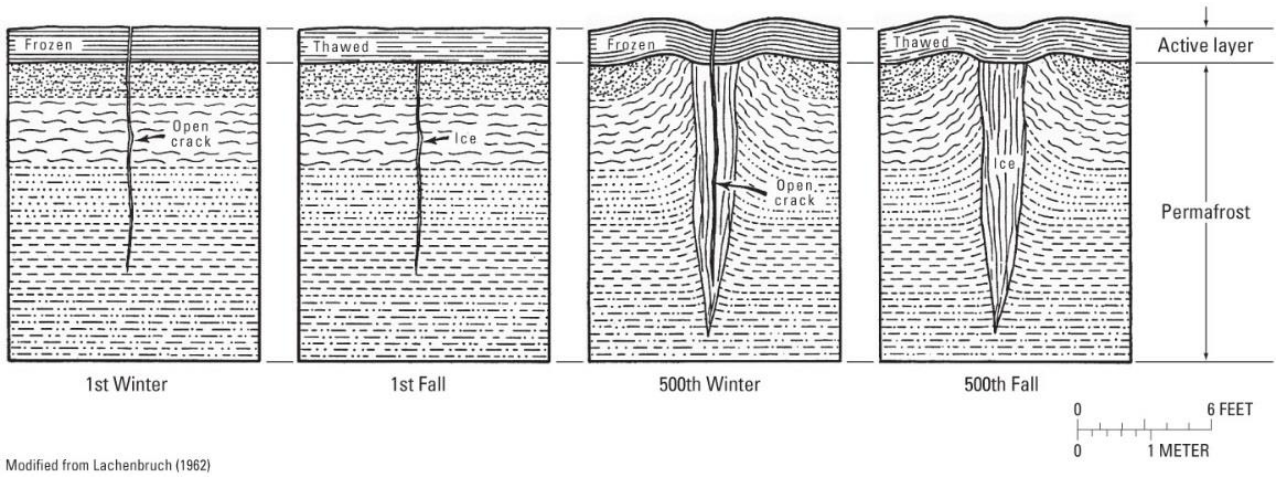

Figure 4. The Formation of Ice Wedges (Lachenbruch, 1962)

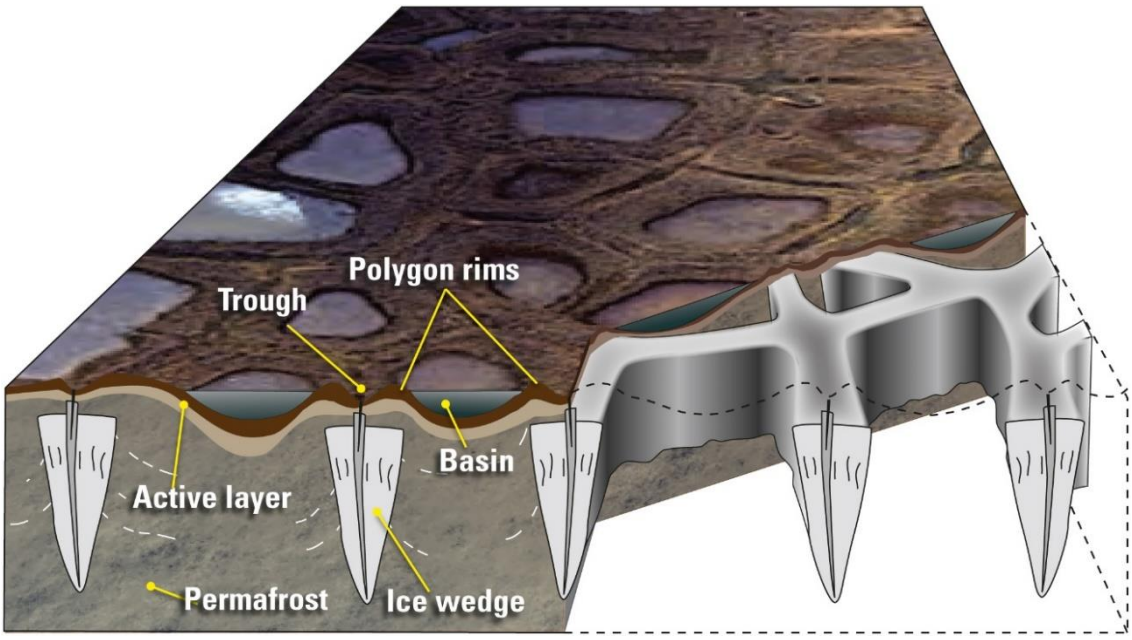

Figure 5. The Surface Expression of Ice Wedges (Martin et al., 2009)

The periglacial terrain exhibits a variety of other patterned ground that is a result of subsurface cryogenic processes. Patterns other than polygons include sorted circles, mounds, and solifluction. Churning of the soil causes fine grained soil to accumulate in the center of the affected area and coarse grain material to form a border around the fines in sorted circles. Mounds in many shapes and sizes are created by heaving of the earth by the expansion of water. Solifluction is characterized by the downward movement of soil on a slope. Solifluction includes frost creep, needle ice creep, and shearing creep (Davis, 2001). The features of permafrost and the related ground patterns have been studied extensively (Black 1976; Davis, 2001; Pewe, 1976; Hopkins et al., 1955); however, the relationship between these patterns and geotechnical hazards is rarely defined in the literature. Corte (1962) completed a study in Northwest Greenland determining the type of ice found under four different patterns that established one of the only documented relationships of ground patterns and subsurface conditions. The observations of his study are shown in Table 1. Using aerial photography to identify patterns and then excavating the site, observations of the ice features were compiled. With only a small sample size, more exploration of the topic is needed, but it provides the basis for understanding the possible hazards that are present with certain ground patterns.

Table 1. Features Related to Four Pattern Types Adapted from Corte (1962).

	Pattern 1	Pattern 2	Pattern 3	Pattern 4
Surface	Network of circles and linear depressions up to 1 m deep	Network of polygonal troughs	Uneven circular patterns with centers of fines and border of coarse material	Low irregular mounds and depressions up to 30 cm deep
Active Layer	No vertical sorting fine grain material with slight accumulation at permafrost table	No vertical sorting of fine grain material	Vertical sorting of fines with accumulation at the permafrost table	Vertical sorting of fines with large accumulation at permafrost table
Ground Ice	Large continuous body of ice with ice wedges in depressions	Well-developed ice wedges up to 1 m wide	Irregular ice masses	Dense concentration of ice masses

Infrastructure Performance on Permafrost

As discussed by Linell et al. (1980), the physical processes that pose the greatest risk to foundations are the melting of permafrost caused by energy transfer from heated buildings and frost action. Melting ground ice can cause a loss of bearing capacity, which can lead to settlement or collapse of soils into large voids. Frost action that leads to heaving of the soil surface and building foundations is similarly destructive. Two major techniques exist to overcome the challenges of building on permafrost. The passive method focuses on the prevention of heat migration from a structure to the ground, and the active method aims to remove the risk of permafrost thaw by replacing thaw-unstable permafrost with non-frost susceptible fill material and insulating the foundation (Muller, 1947). Other less common techniques include compensating for thaw potential with structural tolerances as well as limiting the design life based on permafrost decay (Shankle, 1985). Examples of the passive method

include the use of thermosyphons, Arctic Foundation Air Ducts, and insulation under the foundation.

Many researchers have explored the spatial relationships between building damage and permafrost. Streletski et al. (2012) used existing models of permafrost spatial distribution and climate change to assess the risk of bearing capacity decrease across Russia and compared it to foundation type and performance. Based on methods on Anisimov et al. (1997), they computed the temperature at the top of permafrost (TTOP) and the active-layer thickness (ALT) based on climate, snow cover, vegetation, organic layer of soil, and mineral soils. The results were then analyzed to categorize the change in bearing capacity as the soil warmed. The study concluded that climate changes are expected to continue and that foundations in Russia built with the passive method were more likely to experience damage related to a loss in bearing capacity due to climate change. A similar study from Hjort et al. (2018) used mean annual ground temperature and ALT along with available ground-ice data to assess the risk to infrastructure at the pan-Arctic, concluding that 75 percent of the population faced high risk by 2050 but that high resolution data would be needed to determine the effects at the local level. A survey of Russian cities in the Arctic found between 10% and 80% of structures have been damaged by thawing permafrost as well as 46% of the Baikal-Amur railroad (Kronik, 2001). Similarly, surveys of the Qinghai–Tibet Railway (QTR) in China estimate that up to 40% of the railway has been damaged by permafrost degradation in some sections (Wei et al., 2009). These studies are examples of the use of available data to assess the risks to infrastructure to inform policy but lacks the resolution to inform the decisions of engineers at local levels. Exploring the spatial relationship between infrastructure risk and permafrost requires a focus on smaller areas and at much higher resolution.

Permafrost and Excess Surface Water

Hydrology has a role in many processes of the permafrost terrain, thus making it an important hazard to consider in the built environment (Muller, 1947; Karjalainen et al., 2019). Water influences the aggregation and degradation of permafrost, and permafrost in turn influences the hydrology of a location (Woo, 2012). The focus of hydrology is the hydrological cycle, which is described as the flow of water through many paths in the atmosphere and lithosphere (Chow, 1988); understanding the spatial relationship between infrastructure and this cycle is paramount to characterizing the hazards associated with it. The major risk concerning the crossroads of hydrology and permafrost is the heat capacity of water (1 calorie per gram per degree centigrade). This means that liquid surface water can increase the vulnerability of permafrost to thaw by increasing the thermal conductivity of the ground, which causes a greater flow of heat to the permafrost (Jorgenson et al., 2010; Shur & Jorgenson, 2007). Another destructive property of water is expansion under freezing conditions. When water freezes, it expands by 9%; however, when saturated soil freezes, it can double in volume (Davis, 2001). This expansion is the culprit for frost heave that can produce enough force to lift the foundations of buildings. Regardless of the chosen method of design, building infrastructure on permafrost results in extensive maintenance requirements based on the dynamic environment and the changes unfolding in the northern latitudes (Doré et al., 2016). The dangers of excess water for infrastructure are clear from the body of literature (Linell et al., 1980; Davis, 2001), but the spatial relationship between drainage issues and infrastructure seems unexplored.

Hazard Mapping in the Arctic

Hazard maps are the products of the integration of environmental observations into a simple decision-making tool used to manage the risks related to natural hazards (Benkert et al., 2016). Hazard maps usually refer to those maps created on a community level but representing the spatial distribution of risk that has been accomplished at a large and small scale. Scientists have used active layer thickness, ground temperatures, and satellite imagery to produce risk maps for large areas in the Arctic to understand the possible global consequences of permafrost degradation related to climate change (Brown & Romanovsky 2008; Daanen et al., 2011; Hjort et al., 2018; Karjalainen et al., 2019). These studies help categorize the risk to different regions in the Arctic and provide a tool in the advancement of policy to adapt to changes. Figure 6 provides an example pan-Arctic hazard map communicating risk from permafrost thaw and highlights the need for a closer look at areas such as Northwest Greenland that are not clearly defined. Other researchers have taken a local approach to hazard mapping (Benkert et al., 2016; Flynn et al., 2019; Northern Climate ExChange, 2016; Obu et al., 2019). Researchers based at Yukon College in Canada have conducted in-depth studies of local areas in conjunction with their communities to produce hazards maps to inform community planning and decision-making. With local conditions, such as sunlight, vegetation, and hydrology, playing an important role in the stability of permafrost (IPCC, 2010; Jorgensen & Osterkamp, 2005), detailed studies of small areas are required to understand and communicate risk at a level required for making decisions related to community planning. These studies focus on a framework aimed at tailoring a general methodology to the specific needs of a community, time constraints, and other factors. Figure 7 is an example hazard map made specifically for mitigating the risk from permafrost thaw and other geotechnical hazards through community planning.

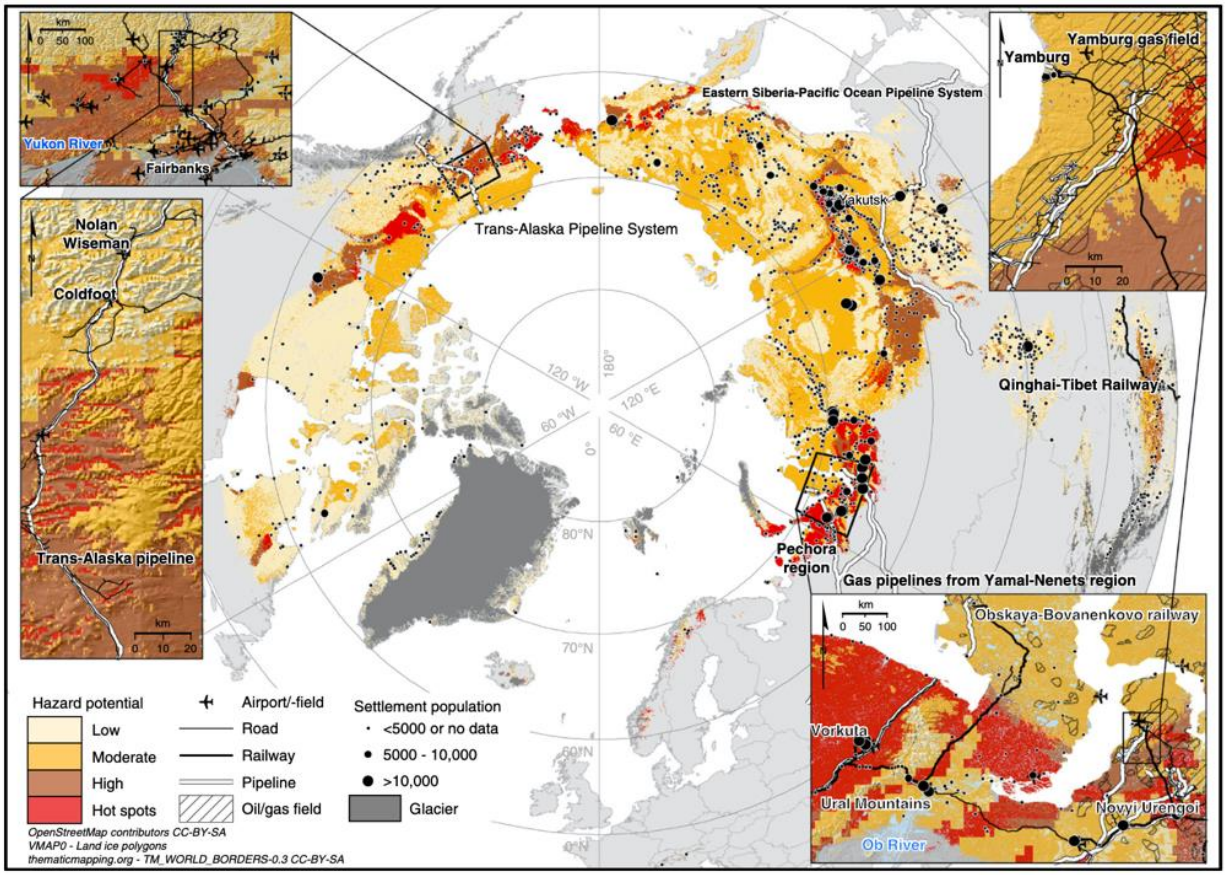

Figure 6. Pan-Arctic Hazard Map Highlighting Risk of Permafrost Thaw (Hjort et al., 2018)

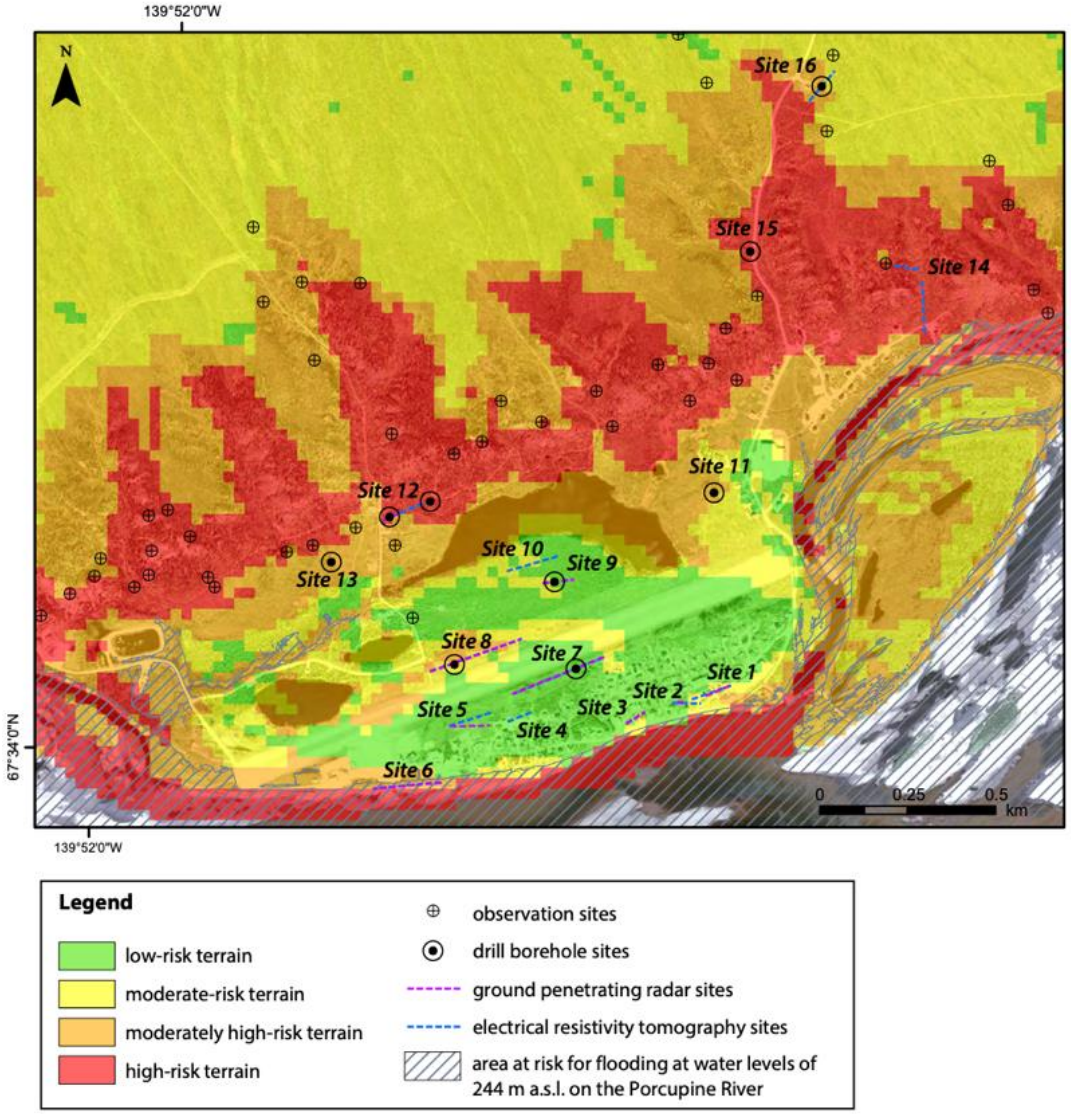

Figure 7. Hazard Map for the Purpose of Community Planning (Benkert et al., 2016)

Common data types used for assessment of permafrost and hydrology include Digital Elevation Models, satellite images, core samples, and ground penetrating radar (Northern Climate ExChange, 2016). Studies such as Benkert et al. (2016) used slope angle, slope aspect, and surface material, with different weights given to each feature to model a cumulative hazard. These studies include extensive site investigation, sampling, remote sensing data collection, and interviewing that increase the power of the map. While the topic of hazard mapping for community planning has been documented in Canada, similar studies are scarce from other sources.

Aerial Photography and Hazard Maps

A major source of data for analysis of permafrost hazards is aerial photography. The use of aerial photography to inform and supplement geologic and geotechnical field work is common (Benninghoff, 1953; Hopkins et al., 1955; Stearns, 1966). Aerial photography can provide a perspective on terrain that is unattainable from the ground or areas that are inaccessible altogether. The use of photos to identify terrain features is not a definitive science and serves only to indicate and inform of possible features, hazards, or anomalies. However, when complemented with an understanding of the climate, geology, and field investigations, photos are important tools for mapping and understanding terrain (Hopkins et al., 1955). Photo interpretation of permafrost features has been a technique used by the United States Geologic Survey and many indicators of permafrost have been documented and studied. Indicators are separated into the major categories of vegetation, polygonal microrelief patterns, features resulting from thawing, and hydrologic phenomena (Hopkins et al., 1955). Each indicator provides specific insight into the ice content, particle size, or hydrologic activity experienced

near the site (Corte, 1962). An important note is made on the limitations of these indicators, emphasizing that they are not conclusive and rely on photo quality and the interpreter's knowledge. These methods for interpreting photos provide another tool to be used in the mapping of geotechnical hazards to construction.

Limits of Hazard Maps

Hazard maps are merely the precursor to in-depth site investigations. Site investigations are crucial to all geotechnical engineering. Understanding soil profiles, hydrology, and geotechnical abnormalities provides information to designers and engineers to determine the strength of soil. One of the main goals of geotechnical engineering design is to distribute the load of a structure across the soil surface so that soil bearing capacity is not reached (Coduto et al., 2016). Identifying soil profiles accurately and to a great enough extent to provide useful engineering properties has always been difficult and costly. The cost and effort required for site investigations prove in many cases to be the limiting factors on the reliability of a design (Ching & Phoon, 2012). Doing the same for permafrost is an even greater challenge. The importance of site investigations and classification cannot be overstated, as it is most often that failures and damage occur because of a lack of understanding of the site. For this reason, site surveys for large areas have been used to give general site characteristics and narrow down the search for acceptable sites as well as provide insights into characteristics that warrant further testing, sampling, or investigation. Aerial photography has been used for many decades to accomplish preliminary site investigations for geotechnical and geologic work performed by the United States Geologic Survey (USGS). For permafrost, the features that exist due to thermal stresses become clues of specific characteristics that can aid in the determination of site hazards.

Thule Air Base

The U.S. Department of Defense (DoD) echoes the concerns of the international community with a call to adapt Arctic infrastructure to climate change and specifically permafrost thaw (DoD, 2020). With critical strategic infrastructure around the Arctic, it is imperative that the DoD continue its research of hazards and adaptation strategies in these areas. While extensive research in cold weather construction occurred throughout the Cold War and continues today in small efforts to mitigate the damage to critical facilities, no effort to understand the modern issues across the DoD's Arctic bases has been undertaken. One of the most important assets, and one with an extensive history of issues related to permafrost, is Thule Air Base. The base maintains billions of dollars in assets, including radars for the Ballistic Missile Early Warning System (BMEWS), also known as the Upgraded Early Warning Radar (UEWR), and satellite control systems, and is poised to continue rising in strategic importance.

Discovery

Thule Air Base is in the Pituffik Valley in Northwest Greenland. With North Star Bay to the east and the Greenland Ice Cap to the west, it inhabits a remote section of ice-free land in the Arctic Circle. The earliest historical mention of the area was in 1849 by a British frigate captain aboard HMS North Star, but the area was already inhabited by locals (Saunders, 1851). In 1910, a native explorer of Greenland set up a trading post named Ultima Thule (Rasmussen, n.d.). In 1946, the United States Marines and other U.S. military personnel established the seeds of the modern base as part of a military exercise called Operation Nanook (Hunt, 1946). Operation Nanook built temporary structures, a weather station, and a dirt landing strip that would kick off

extensive research of the area and lead to Project Blue Jay, the secret construction of Thule Air Base. Figure 8 depicts the location of Thule Air Base.

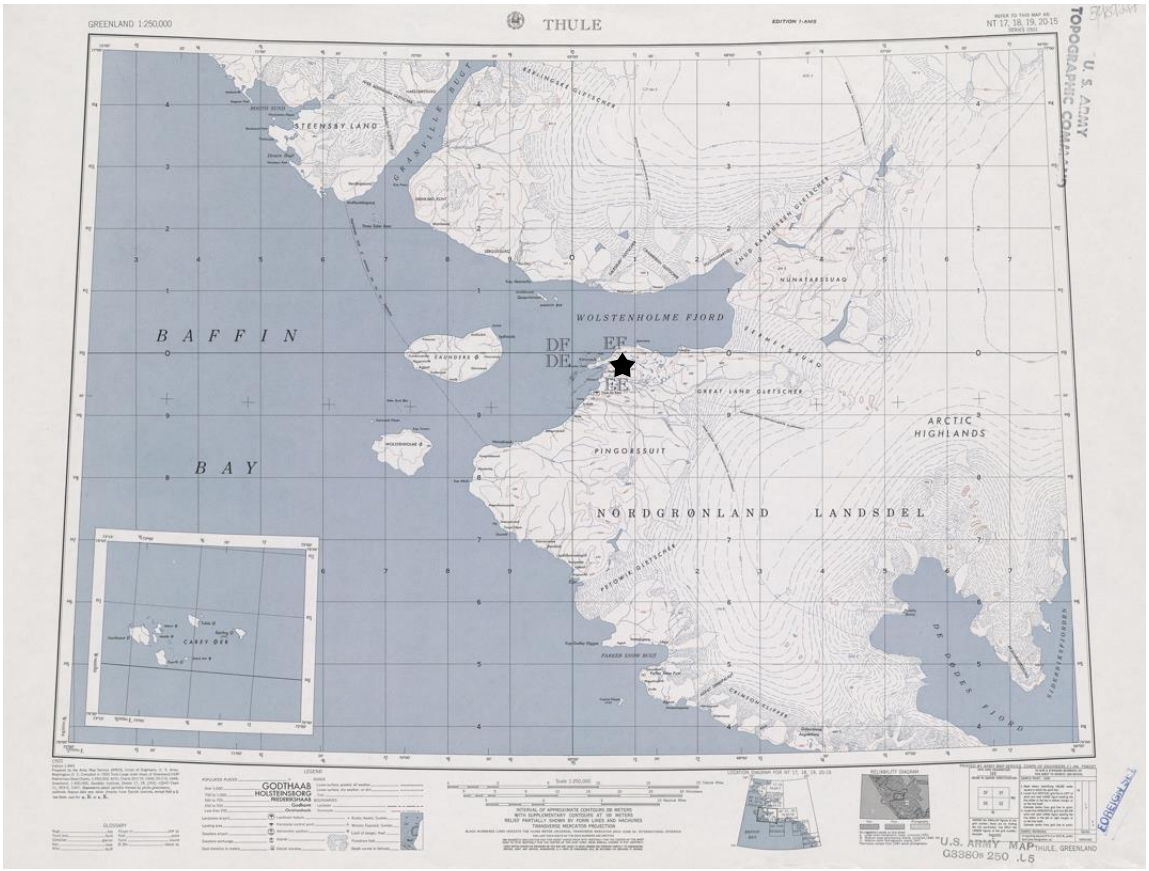

Figure 8. Map of Thule Area (Army Map Service, 1952)

Military History

Based on cold weather challenges experienced during the Korean War, the United States aimed to establish an Arctic base to further deter the spread of communism by the Soviet Union (Dod, n.d.). As the Cold War loomed, Strategic Air Command came to support the idea of a base in the Arctic as a point from which the United States could both launch an attack and watch for an enemy attack. Thule was located 2,800 miles from both Washington D.C. and Moscow. From this idea, Project Blue Jay was born. This project aimed to build a full-scale Air Force

base and operational runway capable of supporting the largest aircraft, in this case long-range bombers, in just a few years. The construction began in July of 1951 and was substantially completed, with the base and runway operational, by 1953. The base continued to expand and focused on building hangars to house bombers and extending the runway to 10,000 feet by 1958 (Dod, n.d.). Thule was designated as the site for the BMEWS in 1960 and remained an emergency landing site for B-52 bombers. In 1982, the base came under the control of United States Space Command until transitioning to the United States Space Force in 2019. The modern mission of Thule remains the operation of the BMEWS as well as serving as a site for the Satellite Control Network, multinational support missions, and scientific research center.

Climate

Thule is located in an Arctic Marine environment, which is characterized by strong seasonality of solar radiation and extremely variable surface features (Bjella, 2015; Walsh, 2008). Temperatures can range from 10°C (50°F) to −40°C (−40°F) with the mean annual air temperature (MAAT) being −11°C (12.2°F) (Bjella, 2015). The area also experiences cyclonic storms in the summers (Dawes, 2006).

Geology and Glaciology

The terrain of the Pituffik Valley is glacially formed and is predominantly composed of sedimentary rocks. The area lies in the Upper Thule Supergroup and is made up of sediment from the Narssarssuk Group and the Dundas Group that are estimated to have formed around one billion years ago in the late Mesoproterozoic to early Neoproterozoic age (Dawes, 2006). It is believed that multiple glacial advances have occurred over the valley between 11.7 and 129

thousand years ago during the Upper Pleistocene Epoch (Founders, 1990). These glacial advances and their eventual retreat shaped the landscape of the valley and deposited 20 ft (6 m) to 60 ft (18 m) of glaciofluvial sill (Bjella, 2018) as well as large amounts of gravel with cobbles and boulders throughout the area (Corte, 1962).

Soil Features

The climate and glacial history of the region created a periglacial environment at Thule supporting the existence of permafrost extending in depth up to 950 ft (300 m) and laterally continuous. The periglacial environment is defined as being not covered by glacier but with the predominant geomorphic processes being frost action (Kaab et al., 2005). The terrain is dominated by matrix (pore) and segregated ice, wedge ice, and relict ice (Bjella, 2018). Active layer thickness ranges from 1 ft (30 cm) under vegetation to 6.5 ft (2 m) in non-vegetated areas, with a transition zone between the active layer and permafrost that is characterized by segregated ice between weathered bedrock (Bjella, 2018), which can periodically thaw.

Built Infrastructure Challenges

The record of infrastructure challenges at Thule began during initial construction of the base in the summer of 1951 and continues today. Most of the modern facility damage has been attributed to poor maintenance of the Arctic foundation systems, inadequate design of insulation, and extreme weather events (Bjella, 2018). Major issues at facilities have warranted in-depth investigations. Soon after the construction of ten hangars on the flight line, severe depressions formed in and around the structures up to 1 ft in depth (Tobiasson, 1970). It was concluded that heat from steam lines, blockages in soil cooling ducts, and foundation fill saturation caused

degradation of the underlying permafrost which was exacerbated by frost action from the saturated soils (Lobucz, 1960). A soil investigation also confirmed a heterogeneous soil system with wedge ice throughout (Tobiasson, 1970). The site of the BMEWS has also drawn much attention. A year after its construction, depressions developed surrounding the site but did not affect the building footprints. It was concluded that disturbance of the glacial debris exposed ice wedges that thawed and eventually the permafrost table stabilized (McAnerney, 1968; USACE, 1964). In November of 2017, changes in floor elevation and buckling of doors and walls were observed, thus prompting an investigation that determined saturation of the fill beneath the foundation and subsequent heaving had caused the deformations, but the permafrost under the main portion of the facility was unaffected. Another portion of the site, the tunnel in Building 4002, was experiencing continual settlement from permafrost degradation due to heating of the tunnel; this was caused by the building not being designed with adequate airflow beneath the structure to be heated. A nearby facility, Building 4016, similarly experienced lateral movement of walls from heaving due to poor drainage and saturation of the fill (Bjella, 2018).

The runway has also experienced deformations since its construction which have been mainly attributed to inadequate depth of fill placed between the permafrost and the runway surface (AFCEL, 1955). Each of the mentioned challenges was analyzed in a reactive manner, with in-depth site investigations completed after damage occurred. Proactive site planning is mentioned in the historical records (Pick, 1953), and additional planning efforts can improve the success and lifespan of future facilities. While field investigations have been completed at Thule, the use of aerial photography to assess landscape hazards is largely unexplored after the work of Corte (1962). The infrastructure challenges thus far have been driven by direct human actions, but the ice-rich soils across the landscape are thaw-unstable and will lose a majority of

their bearing capacity when thawed (Muller, 1947). The next century may bring warmer temperatures and higher precipitation that will jeopardize current and future facilities without proper planning and maintenance.

Summary

A review of the topics related to infrastructure risks at Thule Air Base highlights the need for further exploration of the hazards of permafrost degradation and surface water in the context of the past challenges of Thule and the future development of the base. The analysis of available data will be applied to methods used by previous researchers in the mapping and communication of hazards to help improve the communication between engineers, planners, and decision-makers.

Chapter III. Methodology

The objectives of this researched are achieved through four major tasks. First, the methods to collect and assess weather data for trends is presented. Next, the steps performed to identify, score, and map hazards are outlined, followed by the compilation and recalculation of facility condition scores. Finally, the joining of hazards and facility conditions and the statistical analysis of this product is discussed.

Weather Trend Analysis

The methodology for trend analysis of historical weather data is based on the methods from Lai and Dzombak (2019). The relevant data, chosen metrics, and statistical techniques are discussed in this section. The goal is to compare the statistical and visual trends of historical weather data to climate projections.

Data Collection

Historical weather data is available through the National Oceanic and Atmosphere Administration but was supplied from the Thule Air Base Weather Flight and the 14th Weather Squadron. The data includes daily maximum, minimum, and average temperature; snowfall; and precipitation. The data covers 1951 to 2020 but is missing temperature for 1970 to 1975. The data is provided in single-day intervals and was converted to the desired metrics using Microsoft Excel. Many metrics are used to describe the temperature and precipitation patterns in different regions of the world. One common metric for the Arctic is Mean Annual Air Temperature (MAAT). This metric is relevant to this study because it helps indicate the likelihood or risk of

permafrost decay and the transition between continuous and discontinuous permafrost (Smith et al., 2002). Categorizing the temperature of a location by an annual average gives a simple measure of the likelihood that frozen ground will stay frozen throughout the year. To achieve this metric, the SUMIFS statement is used in Microsoft Excel to sum all average daily temperatures that fall within the given year. This number is then divided by the number of days in that year. Another important metric is total precipitation. Precipitation has an important impact on drainage hazards and can raise the thermal conductivity of the ground (Douglas et al., 2020). Extreme precipitation events in recent years have also been indicated as major contributors of infrastructure damage; additionally, heavy snowfall can contribute to a buildup of snow around facilities that can melt and infiltrate the fill below the foundation (Bjella, 2018).

Statistical Analysis

Ordinary Least Squares regression was the chosen method for testing the positive trend in temperatures and precipitation at Thule Air Base. In order to guide the discussion of trends, the available data was analyzed on a decade, two decade, and lifetime basis. Similar to Lai and Dzombak (2019), a 10-year moving average was applied to accomplish this comparison. This sets each decade apart from the previous decade and allows for comparison between decades to help identify trends hidden by natural variability across time.

The first step for completing any regression is to test the assumptions of the model. In this case, there are four assumptions for basic linear regression: the mean of the residuals is 0, the variance of the residuals is constant, the data is normally distributed, and there is no auto correlation (residuals are independent). These assumptions are shown in Table 2 and were tested in Python. After the assumptions are tested, a linear model is fit to the available data. This model created a

line that minimizes the square root of distances between the line and all points. The slope of this line provides a measure of possible trends, and the correlation coefficient describes how well the model explains the data.

Table 2. Assumptions of a Linear Model Tested in Python.

Assumption	Test (In Python)	Desired outcome
Mean of residuals = 0	Plot and visual inspection	Mean is centered around 0
Variance is constant	Breusch-Pagan	High P-Value (>0.05)
Normally Distributed Errors	Shapiro-Wilk	High P-Value (>0.05)
No autocorrelation	Durbin-Watson	Value between 1 and 3

Hazard Mapping

Identification and visualization of hazards at Thule Air Base is accomplished using ESRI's Geographic Information System ArcMap. Data is collected from online sources and first used to identify the hazards present. Scores are given to each hazard to create individual hazard maps for each category before creating a cumulative map to visualize the geographic distribution and severity of all hazards.

Data Collection

The first step in surface analysis is the collection of remote sensing data for the area of interest. The data for this analysis was obtained directly from the Civil Engineer Flight at Thule Air Base. File size of remote sensing data can make transfer challenging, and this was overcome by mailing the data on a hard drive. The data was collected in 2018 by a third party under Air Force contract in which Light Detection and Ranging (LiDAR) scans of the base were performed at a 0.5-meter resolution and orthometric imagery was collected at 7.5 cm resolution. This data

included point clouds, Digital Elevation Models (DEM), and orthometric imagery; only the DEM and imagery were analyzed. This data is also available to all Common Access Card (CAC) holding Department of Defense (DoD) employees on a government network through the site https://maps.af.mil. By entering the Map viewer on the home page and then navigating to the bookmark tab and the data catalog button on that tab, the data can be searched in the Air Force database. It is important to read the user agreement for this data.

The primary data source for mapping the hazards at Thule Air Base is high resolution aerial photography, both modern and historical, and DEM files. Generally, studies mapping ground hazards include other sources such as field investigations and ground penetrating radar, but the scope of this study is limited to the visual analysis of the available aerial photographs and the analysis of the DEM files (Northern Climate ExChange, 2016). Along with DEM and imagery, limited aerial photographs from 1952 are available from the Danish Geodata Institute. Historical aerial photography is also available at the National Archives but was unavailable during this study.

Hazard Identification and Mapping

The hazard map developed in this study is based on the hazard sources of drainage pathways, ground slope, and visible permafrost features. It is important to note that these methods are based on ESRI's ArcMap 10.7.1 with the Spatial Analyst license activated. Other versions of ArcMap may perform analyses differently and contain different inputs and outputs. The workflow of this methodology is visualized in Figure 9 and described below.

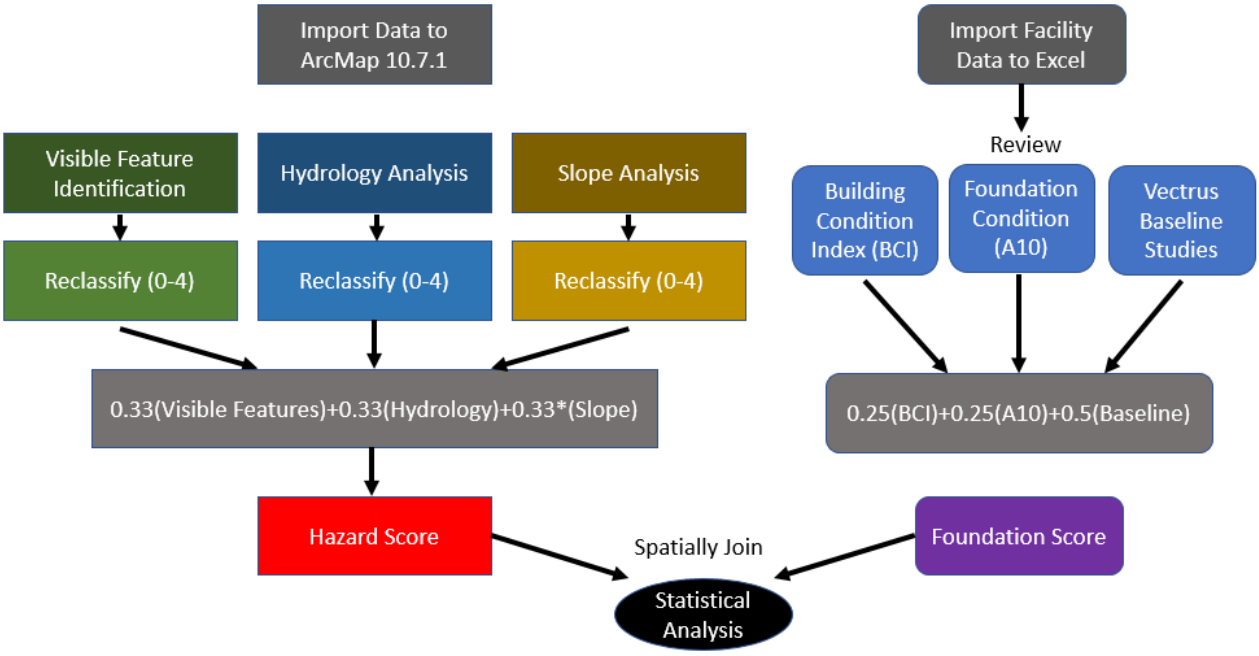

Figure 9. Methodology for Hazard Identification and Foundation Assessment

Identifying Drainage Pathways

The Hydrology tool kit in ArcMap was the main resource used to identify and visualize the hydrology of a site. The use of these tool begins with the import of the DEM. The file type of a DEM can vary, but ArcMap will recognize many of the formats and import them as a raster file. The data for Thule includes varying resolutions but for this research 1-meter resolution was used. For an area as large as an Air Force base, this file is too large for a standard home computer to handle; therefore, the aggregate tool was used with a cell factor of 4. This took the 16 closest cells and averaged the elevation to create a single cell. Although this decreases the accuracy of the outputs, it also decreases the computation time and prevents crashing of the application.

The next step in the process of preparing the raster file for analysis is the fill tool. The fill tool identifies sinks in the data, which are points that are surrounded by higher elevation points. This allows for simulation of flow because when sinks are not filled the cell will not accumulate into the next cell. The z-limit sets the limit of the sink depth; it is important to understand that without a specified value, all sinks will be filled. For the first iteration, all sinks were filled using no z-limit to simulate the wetland conditions experienced at Thule. Next, the flow direction tool was run to model the flow from each cell to the steepest downslope neighbor. Three models are available; in this case, D8 was selected to compare each cell to the eight nearest neighbors. Finally, to generate a raster of drainage paths, the flow accumulation tool was run. This tool accumulates the weight of each cell generated by the D8 model and outputs a raster file. The raster calculator can be used to filter the desired values. In this case, trial and error created three different raster files with a limit of 1,000, 5,000, and 10,000, respectively. The goal is to model drainage patterns under different conditions such as dry, light rain, or heavy rain. The limit values are arbitrary to achieve a similar density of drainage paths to those visible from imagery. These values represent the number of cells that drain into the given cell.

Identifying Ground Slope

Slope analysis was accomplished using the 3D analyst tool kit. The slope tool within this toolkit accepts any raster file with elevation data and the output can be specified as angle or slope percentage. For this research, angle is specified as the output. The tool uses the provided elevation data to compute the angle between each cell. Slope is identified as a hazard based on its influence on slope stability and the movement of earth on slopes due to cryogenic processes (Davis, 2001).

Identifying Permafrost Features

Permafrost features can be identified through photogrammetry, which is the interpretation of photography for information. Using descriptions from permafrost experts and texts, the researcher scanned the available images for features matching the descriptions of common visible landscape features of permafrost terrain. The visual identification of features was based on Davis (2001) and Corte (1962). These resources provide examples of the identifiable features in permafrost regions (Davis, 2001) and Thule Air Base itself (Corte, 1962). Corte (1962) identifies the four major patterns shown in Table 3. The descriptions of surface cues and subsurface explorations were used to identify each feature and validate that it poses a hazard. The proximity of the study area in Corte (1962) to the focus of this research, shown in Figure 10, increases the likelihood that the features he described may be similar to the ones identified in the current study. Figure 11 shows an aerial photo from Corte (1962) that was used as a point of comparison to the features described in his study and to the features identified in the current study.

Table 3. Patterns Investigated near Thule Air Base (adapted from Corte, 1962).

Pattern	Description
Type 1	Depressions in the form of kettles or valleys of about 1 m relief in coarse unsorted gravel and sand spaced from 6 to 10 m on centers.
Type 2	Very well-known ice-wedge polygon. In the Thule area these polygons commonly have a mesh diameter of 20 to 30 m.
Type 3	Sorted circles or centers of fines surrounded by coarse washed particles. There is a wide size variation in those observed around Thule. Ranging from a few centimeters to several meters in diameter.
Type 4	Elevations and depression of low relief, without surface sorting. The humps in this pattern are flatter and less well developed than those of type 1 and are formed by finer material. Vegetation growing in the depressions outlines the mounds more distinctly.

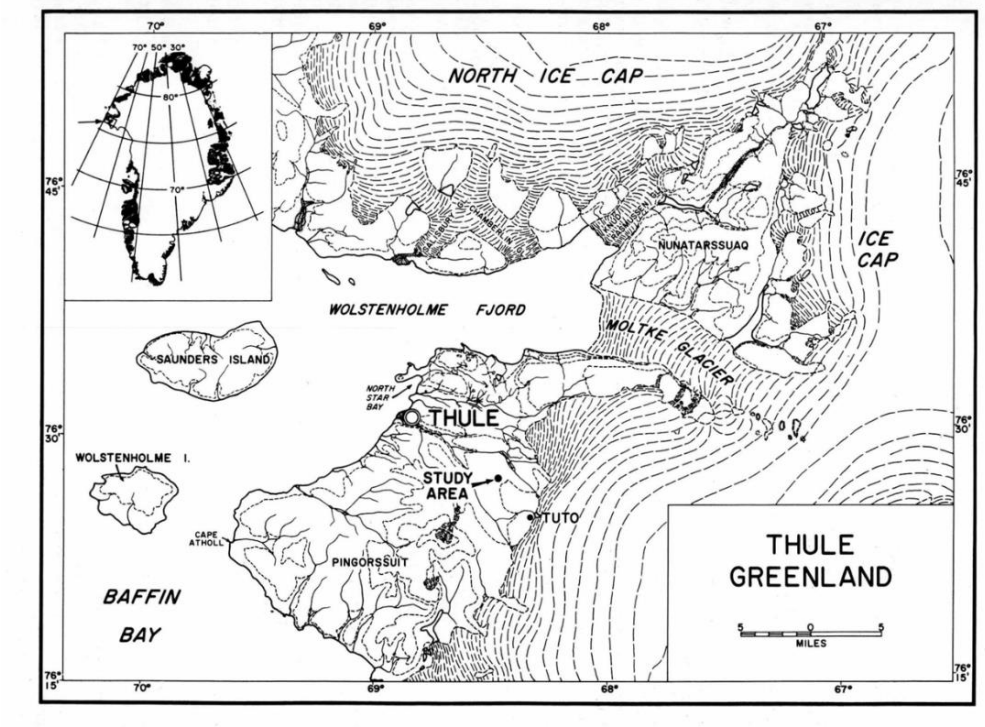

Figure 10. Location of Permafrost Investigation near Thule Air Base (Corte, 1962)

Figure 11. Aerial Photograph of a Study Near Thule Air Base (Corte, 1962)

Detailed descriptions of cryogenic landforms and process from Davis (2001) and Black (1976) were also used to identify features. A two-step process described in Ray (1960) was used to catalog the features of the base. This process involves first observing and cataloging features and second using inductive and deductive processes to determine the significance of the feature. In order to keep track of locations that are scanned, the researcher scanned from east to west starting in the southwest corner of the photo. These scans were completed at three different extents initially: 1:1,000, 1:5,000, and 1:10,000. These extents can be manually set in the extent dropdown in the tool bar or using the scroll wheel on a mouse. Examples of these extents are shown in Figure 12.

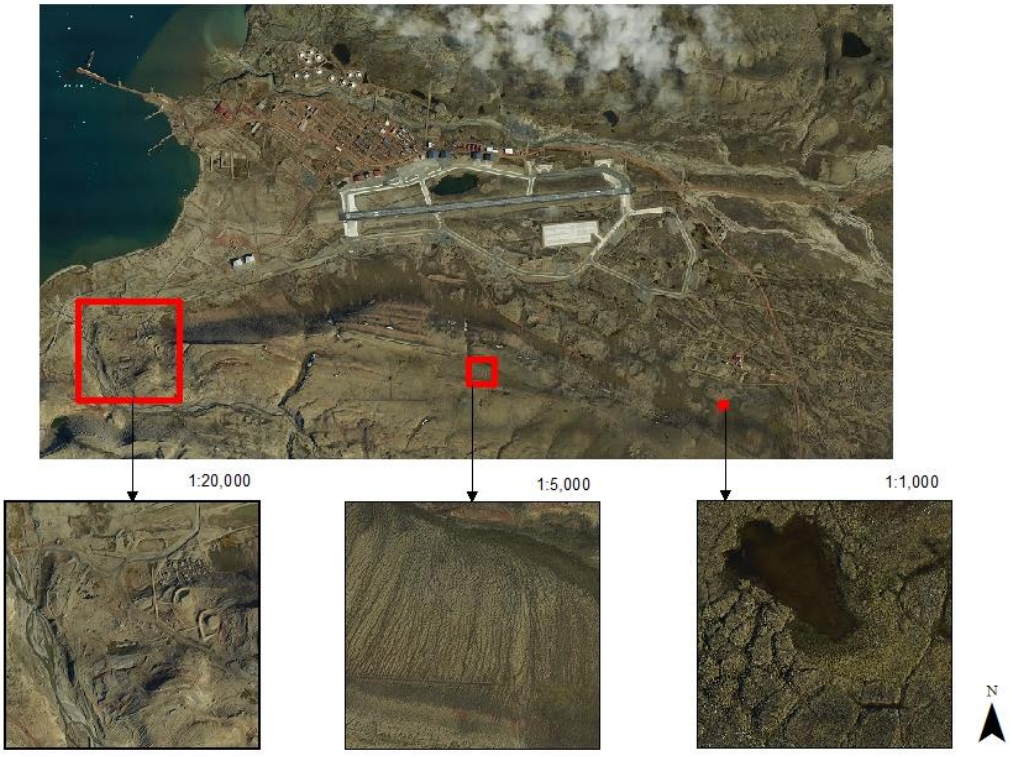

Figure 12. Visualization of the Scanning Extents

This approach also allows for the identification of features from different perspectives, as some features will only be identifiable from an extreme zoomed view and some from a more removed perspective. If a feature spans outside the given extent, the feature is followed to the next extent and identified, then the scan begins again from the previous extent. Although a system was created to scan the photos, the process is inherently iterative, as it is possible to identify other features that were missed during the previous iteration. Before importing the data to be analyzed, a database was created to catalog the features that were identified. In the catalog window of ArcMap, an existing geodatabase was chosen to store the features. By right clicking on the database, a new feature dataset was created named "permafrost." Within this dataset, feature classes were created for each unique terrain feature. As the scan is completed, the freehand tool within the editor window was used to outline the visible features and add them to the respective feature class. The feature classes include, polygons, sorted circles, mounds, solifluction, ponding, and historical versions of each to differentiate those identified from historical photos.

After scanning and cataloging the photography from 2018, the available historical imagery was imported for analysis. Since this imagery is not geographically referenced, the georeferencing tool in ArcMap was used. Once the image is imported, it can be moved to the desired extent for comparison to the modern images. The georeferencing drop-down provides this capability. The process begins by studying the two photos for identifiable similarities. Using the ESRI (2020) guidelines for georeferencing, the control points were chosen by searching for features such as rock outcroppings, road intersections, and jetties of land. Based on the nature of each photograph, a different number of control points was required for the program to accurately orient or warp the photo; however, more control points do not ensure a better result

(ESRI, 2020). Once the control points were added, the photo was saved with its georeferenced data for continued use.

An example photo georeferenced for this study is shown in Figure 13. Permafrost features, large rocks, and road intersections are the most available features at Thule for georeferencing. If three control points were chosen and a fourth distorted the photo, then it was removed and only three were kept. When comparing photos of different resolution, and landscapes that have undergone significant erosion such as Thule, extra control points can warp the photo out of alignment. Once georeferenced, the photos were scanned for permafrost features. If a feature was previously identified on the modern photograph, the historical feature will leave out the modern section, unless the feature is ponding and the ponding has increased in size.

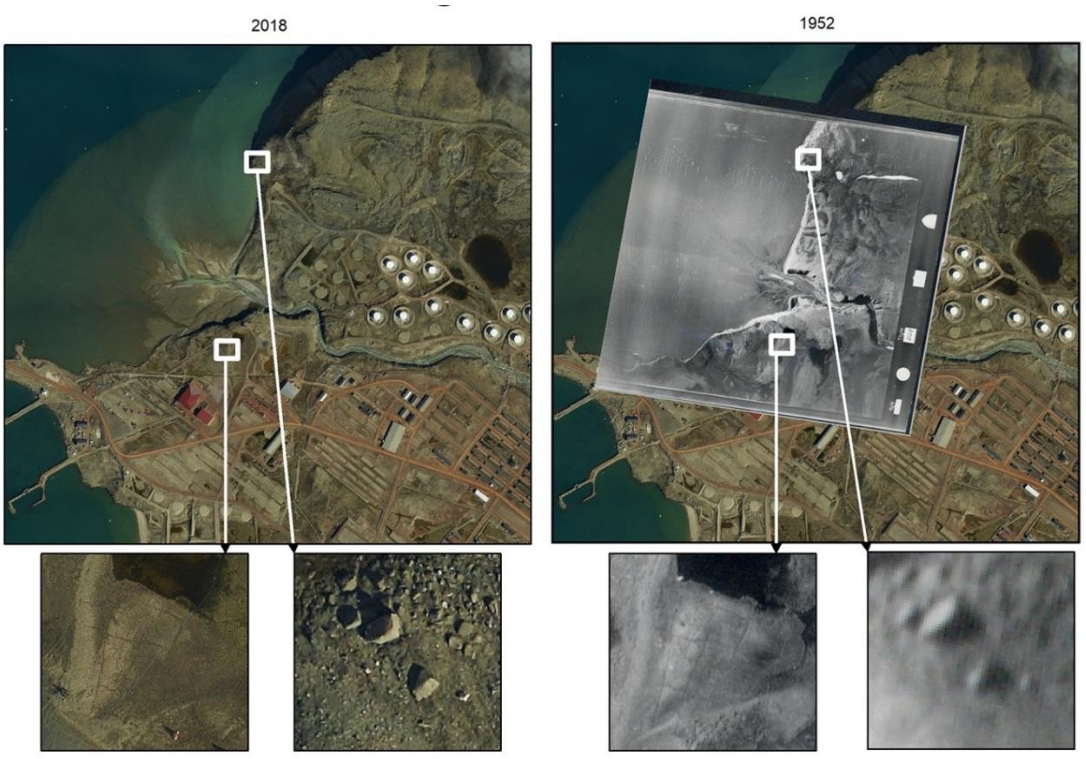

Figure 13. Example Features Used to Georeference Historical Photos

Hazard Scoring and Map Creation

The identified features are given a score to reflect the level of hazard they pose to infrastructure. The data transformations are provided in Table 4. Based on the subjective nature of identifying these hazards, the scoring system was simplified to a 1 to 4 scale, indicating low to high hazard to infrastructure. Drainage is a significant hazard to infrastructure based on the threat of thawing permafrost and the ability to damage foundation through frost heave if the fill becomes saturated. The categories were scored based on raw cell accumulation data; very low, low, medium, and high drainage accumulation are therefore given scores of one, two, three, and four, respectively, on the hazard scale. Slope was reclassified from raw angles and given hazard scores of 1 to 4 using natural breaks provided by the ArcMap software. The permafrost features are manually scored based on the nature of the degree of threat to foundation health. Once scoring is complete, a map of each feature category is created followed by a cumulative map of the hazards. Each hazard is given an equal weight and the cell statistics tool is used to create a final hazard score. For each map, the color red is used as the sole indicator of hazard, with a darker color indicating a greater hazard. Equation 1 is used to create the final hazard score, where P is the permafrost hazard score, D is the drainage accumulation hazard score, and S is the slope hazard score.

$$Cumulative\ Hazard\ Score = 0.33P + 0.33D + 0.33S \quad (1)$$

Although a non-equal weighting could be rationalized for these variables, this research does not account for other factors that would justify something other than equal weight. Using the methods and reasoning presented, each category presents a hazard to infrastructure and its

severity is captured in the scoring system. Researchers like Benkert et al. (2016) justify non-equal weightings such as a 60% weighting of surface materials in their model because of the significant impact this category has on stability and the link to permafrost features and drainage.

Table 4. Hazard Scoring

Feature	**Raw Classification**	**Hazard Score**
Very Low Drainage Accumulation	0-1000 cell accumulation	1
Low Drainage Accumulation	1000-5000 cell accumulation	2
Medium Drainage Accumulation	5000-10000 cell accumulation	3
High Drainage Accumulation	10000+ cell accumulation	4
Very Low Slope	0-12 degrees	1
Low Slope	13-25 degrees	2
Medium Slope	25-45 degrees	3
Steep Slope	45+ degrees	4
Solifluction	Visual	1
Ponding	Visual	2
Sorted Circles	Visual	3
Mounds	Visual	3
Ice Wedges	Visual	4

Foundation Condition Assessment and Mapping

The final task in building an understanding of the relationship between the distribution of hazards and the damage to foundations is the quantification of this damage and joining it to the geographic facility data. Rather than relying only on the building condition index usually available for facilities, a composite score of multiple sources is created. Once a score is calculated, it is joined to the building footprints in ArcMap and finally spatially joined to the hazard data.

Creating a Composite Score

Three values contributed to the final foundation damage score: Building Condition Index (BCI), or the overall facility health; the Foundation Condition Score, a value provided in column A10 of BUILDER; and a score created by the researcher from the baseline facility inspections completed by the base maintenance contractor (BMC) in 2017. To create a compatible score based on facility inspection data, each report was reviewed for damage related to the foundation. This included comments on the foundation, the interior floor, the interior and exterior walls, and the drainage around the facility. As shown in Table 5, four codes are used to characterize the facility condition (Thule Base Maintenance Contract, 2017). A final score is created using Equation 2, where BCI is the Building Condition Index provided in the BUILDER report, A10 is the foundation condition provided in the BUILDER report, and B is the score resulting from the baseline assessment by the BMC.

$$Foundation\ Condition = 0.25BCI + 0.25A10 + 0.5B \quad (2)$$

Table 5. Codes and Descriptions used in Inspections.

Code	Name	Description	Foundation Damage Score
C0	No Comments	The item is assessed to be in a fully satisfactory functional condition, equivalent to its designated purpose or to new equipment of the same type.	100-90
C1	Less serious wear/cosmetic wear	The item is assessed to be in a condition equivalent to its designated purpose and with deterioration equal to fair wear and tear or worn only to such a degree that it has no influence on the function of the item. Therefore, no repair or overhaul is considered necessary.	89-75
C2	Serious wear	The item is assessed to be in a condition only less equivalent to its designated purpose and with deterioration beyond fair wear and tear or worn to such a degree that it **may** fail within a few years. Therefore, repair is considered necessary within a measurable time.	74-50
C3	Critical wear	The item is assessed to be in a condition not equivalent to its designated purpose and with deterioration beyond fair wear and tear or worn to such a degree that it **will** fail within a short period. Therefore, repair must be planned and carried out as soon as possible.	49-25

Based on the frequency of these codes and the comments that accompany them, a new score was assessed to the facility ranging from 100 to 25 with lower numbers indicating more damage. After scores were assessed for each facility, the three scores were combined with a BCI:A10:Baseline ratio of 1:1:2. The baseline score is weighted twice that of the BCI and A10 column because it is based on detailed reports that include specific comments on the foundation and foundation-related damages; additionally, it is validated with pictures taken by the BMC (not

provided in this report). The BCI and A10 scores are numbers without any documentation or known timeframe of inspection. Finally, the scores were reviewed for accuracy by the base civil engineer at Thule Air Base. These scores are joined to the shapefile of building footprints based on the building number.

Mapping

Once these data were finalized, it was spatially joined to the building footprints. Building footprints are available through https:\\maps.af.mil and can be downloaded from the geodatabase of Thule features. A raster-to-point conversion is necessary to create a compatible layer to spatially join hazard scores and facility data. The operation of converting a raster to points is computationally heavy; based on the extent of the data and the chosen resolution, it will create millions of points. Before spatially joining the data, the building footprint was expanded to simulate the horizontal extent of soil considered by a geotechnical engineer in designing a foundation (Coduto et al., 2016) and due to the nature of visual identification of ground features being speculative and imprecise (Ray, 1960). The buffer tool was used to increase the footprint by 5 meters on each side. The final step was to spatially join the hazard points to the building layer. The option to compute a statistic of the values within the boundary of the polygon is available. The sum, average, and maximum provide the total sum of hazards under the chosen footprint, the average hazard per area, and the maximum hazard score under that footprint.

Statistical Analysis

To explore the relationship between the hazards and the foundation score, a statistical analysis of the hazard scores and foundation conditions is completed in Python. This process

includes calculating the descriptive statistics of the dataset, completing simple linear regression, outlier removal, data transformations, and further regression to discover if a relationship exists between variables. The primary goal is testing statistical models for their fit to the calculated data. First, average hazard score, average foundation condition, and the 10 facilities with the highest hazard are calculated in Microsoft Excel. These metrics stand alone as a way to describe the hazard to base infrastructure regardless of the manifestation of damage related to these features and identifying specific facilities that are at high risk. These metrics also allow for the identification of outliers. Next, the data is imported to Python for analysis. After the assumptions of linear regression are tested, iterative regression is completed on transformed versions of the dataset.

ArcMap

The methodology presented relies heavily on an understanding of the tools and workflow of the ArcMap 10.7.1 software. A detailed guide to the ArcMap tools used is included in Appendix C. The general flow of the methodology in the context of ArcMap is provided below.

1. Import relevant data into the desired layer in the table of contents
2. Perform any necessary transformation and georeferencing to use the data for analysis
3. Create separate feature classes in a chosen geodatabase to catalog the visible features
4. Analyze the available data for the chosen hazards using available ArcMap tools
5. Convert features to rasters, and covert each hazard from its raw classification to a hazard score using the raster reclassification tool
6. Convert the final raster to points using the raster to points tool
7. Combine rasters using the cell statistics tool

8. Join facility condition data to available shapefile of buildings using the join based on table option
9. Join facility layer to hazard points using the spatial join option and specify desired mathematical outputs.

The specific tools and options within the toolkits are dictated by the desired outcome, the computing power, and the resolution of available data. A basic understanding of the ArcMap's internal calculation can assist in the creation of the desired outcome. Each tool has documentation on the ESRI website (https://desktop.arcgis.com/en/arcmap/).

Chapter IV. Results and Analysis

The results and analysis section first presents the results of the statistical analysis of temperature and precipitation and suggests the implications of these results. This discussion is followed by the presentation of the identification and mapping efforts for visible terrain, drainage and slope related hazards along with the accumulation of these hazards, and discussion of the distribution of these hazards. Next, the results of the foundation damage assessment and subsequent joining with hazard data and statistical analysis is discussed. Finally, a summary captures the significance of the analysis as a whole.

Climate Trends

As shown in Figure 14, a visual inspection of the Mean Annual Air Temperature (MAAT) at Thule Air base from 1951 to 2020 indicates a gradual decrease in temperature from 1951 to 2000 and a drastic increase in the two decades leading up to 2020. These visual trends support the claims that the Arctic has experienced higher than average warming in the past two decades than the rest of the world (IPCC, 2019) and that gradual warming suggested by 14th Weather Squadron's projections may have underestimated the drastic changes that have occurred. These trends also correspond to an increase in investigations conducted at Thule for facility damage related to foundations (Bjella, 2015; Bjella, 2018).

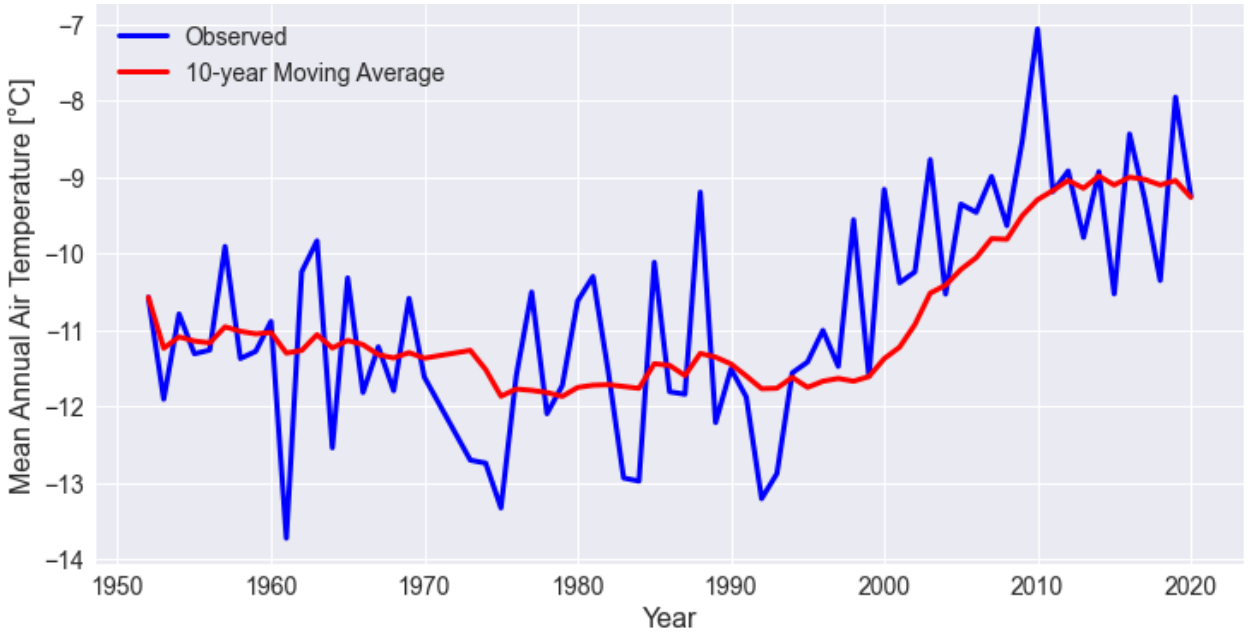

Figure 14. Mean Annual Air Temperatures and Moving Average

The results of the Ordinary Least Squares (OLS) regression indicate an average increase of between 0.025 and 0.05 degrees Celsius per year for the last 68 years, with an R-squared of 0.295 and a 95% confidence level. The model shown in Figure 15 is statistically significant with a p-value less than 0.05, which suggests a moderate positive correlation between the MAAT and the year. These results support the conclusion that there is an increased risk of changes to the thermal balance of the terrain based on increasing air temperatures and that weather-related design parameters must be updated to improve the lifespan of facilities. This also indicates an increased risk to current and future infrastructure if maintenance and community planning efforts are not undertaken. The 10-year moving average, seen as the red line in Figure 14 additionally supports the interpretation of a more drastic warming over the past two decades in particular. This observation is supported by similar observations that coastal permafrost began degrading significantly in the early 2000s as a result of increased air temperatures and decreased sea ice (Thoman et al., 2020).

DV	MAAT
IV	Year
Observations	67
R-Squared	0.295
Model	Ordinary Least Squares
Model P-Value	0.00000205
Equation	MAAT = 0.0382 *(Year)- 86.6
Coefficient P-Value	0
Intercept P-Value	0

Figure 15. Model Outputs and Line of Best Fit for MAAT

From 2010 to 2015, the 14th Weather Squadron used the CMIP5 climate model to create climate projections for Air Force bases around the world. Based on the worst-case scenario for global greenhouse gas emissions, named by climate scientists as Representative Concentration Pathway (RCP) 8.5, the MAAT for Thule Air Base was projected to be -8.33 degrees Celsius for the year 2030. Based on daily measurements from the Thule Air Base weather station, the MAAT for 2019 was -7.9 degrees Celsius, the second warmest year on record behind -7.06 degrees Celsius in 2010. These observations suggest an underestimate in climate projections and support the conclusion that rapid change is occurring in the Arctic as a whole and specifically for the region of Thule Air Base. With thermal balance being essential to the stability of permafrost (Davis, 2001; Muller, 1947) and rising temperatures leading to a reduction in sea ice and increase in precipitation (IPCC, 2019; Ballinger, 2020), it is imperative that engineers base designs on updated climate projections to ensure facilities can perform for their designed life.

Precipitation data for Thule Air Base is only reliably available from 2000 to 2020. Given this short range of time, no recognizable pattern is apparent in the data. Figure 16 provides a visualization of the total precipitation in millimeters for a given year and the orange line represents the 10-year moving average. This moving average indicates no observable changes in precipitation patterns in the last 20 years. Additionally, the model outputs shown in Figure 17 show that the data does not fit to a simple linear model. The sporadic nature suggests that a model may not fit the data. Obtaining more historical data would be important to determining a possible pattern. Based on these results, it is difficult to speculate on a trend regarding precipitation; however, based on decreasing sea ice levels and the rising temperatures, it is anticipated that increased precipitation would follow. The projections prepared by the 14th Weather Squadron indicate that precipitation may decrease over the next few decades, contradicting the presented rational and indicating that more investigation into precipitation trends and projections is needed. Although an obvious trend is not discernable from the precipitation data presented, a pattern of extremes is visible as each year varies wildly in precipitation totals. This pattern may raise the risk to facilities based on a buildup of snow, possible flood events, and the difficulty to predict the need for maintenance and remediation of drainage around facilities.

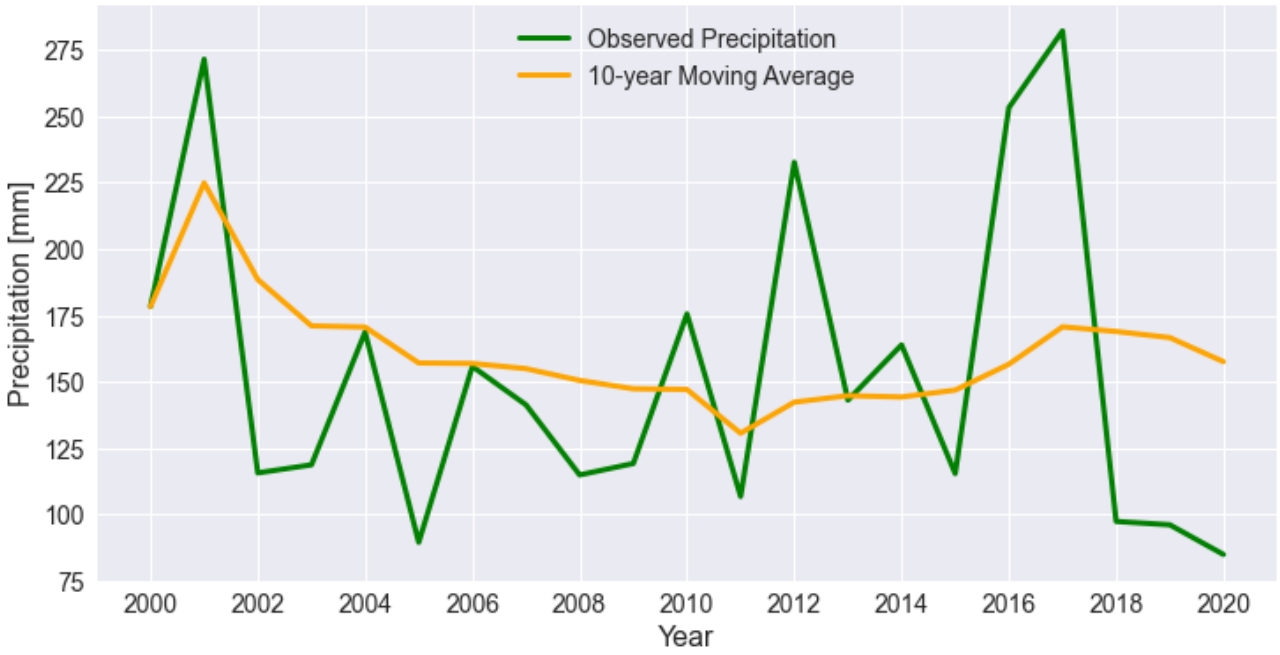

Figure 16. Annual Precipitation Totals

DV	Precipitation
IV	Year
Observations	21
R-Squared	0.007
Model	Ordinary Least Squares
Model P-Value	0.722
Equation	PREC = -0.8 *(Year) - 1765
Coefficient P-Value	0.697
Intercept P-Value	0.722

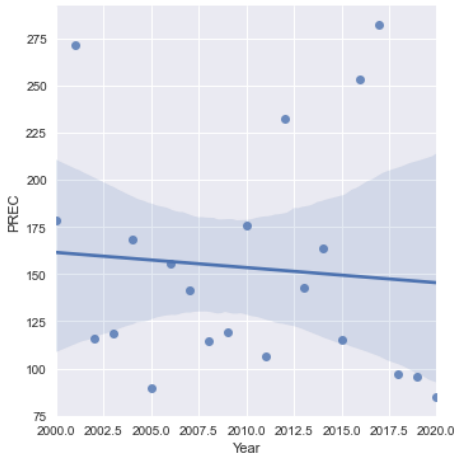

Figure 17. Model Outputs and Line of Best Fit for Precipitation Data

Hazard Identification and Mapping

The analysis of photographs and DEM files indicates that hazards are present across the available data range. Visible permafrost features, drainage hazards, and slope hazards are identified in separate maps, as well as in a cumulative map. The results of mapping the hazards and scoring them is included in this section.

Visible Features

Permafrost features are abundant across the landscape and throughout the developed areas of the base. Five major categories were identified as shown in Figure 18: ponding (A), solifluction (B), mounds (C), polygons (D), and sorted circles (E). Over 450 separate items were identified, with a majority of the items representing ponding due to the sporadic nature of the feature. Figure 19 illustrates the distribution of feature types. Solifluction dominates South Mountain suggesting that cryogenic action is moving the slope of the mountain downward. Mounds are abundant at the base of South Mountain possibly from saturated fine grain soils heaving and creating protrusions. Polygons are clustered around the coast in the industrial area of the base, and ponding is visible all across the valley and on the mountain sides suggesting saturated soils and possible thawing permafrost. Much of North Mountain is obscured by clouds in the photographs and limits identification of features, but few facilities are on North Mountain and the LiDAR data was not obstructed. These results support the conclusions of Bjella (2018) that the valley has many massive ice features that are often random in nature but also are influenced by water sources, as shown by the abundance of ice wedges near the river delta, ice wedges in the valleys of South Mountain, and features such as sorted circles in well drained areas such as the western slope of North Mountain.

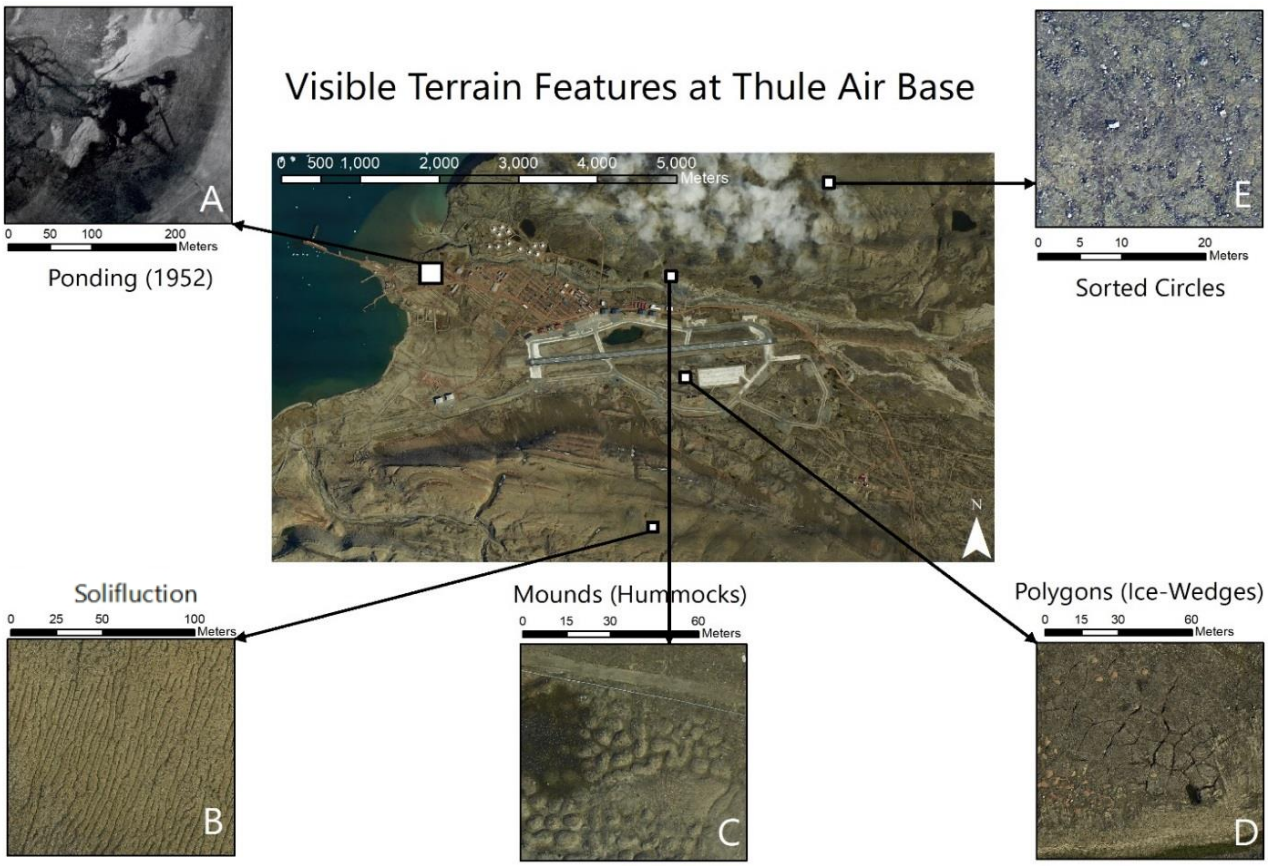

Figure 18. 5 Major Features Identified from Imagery

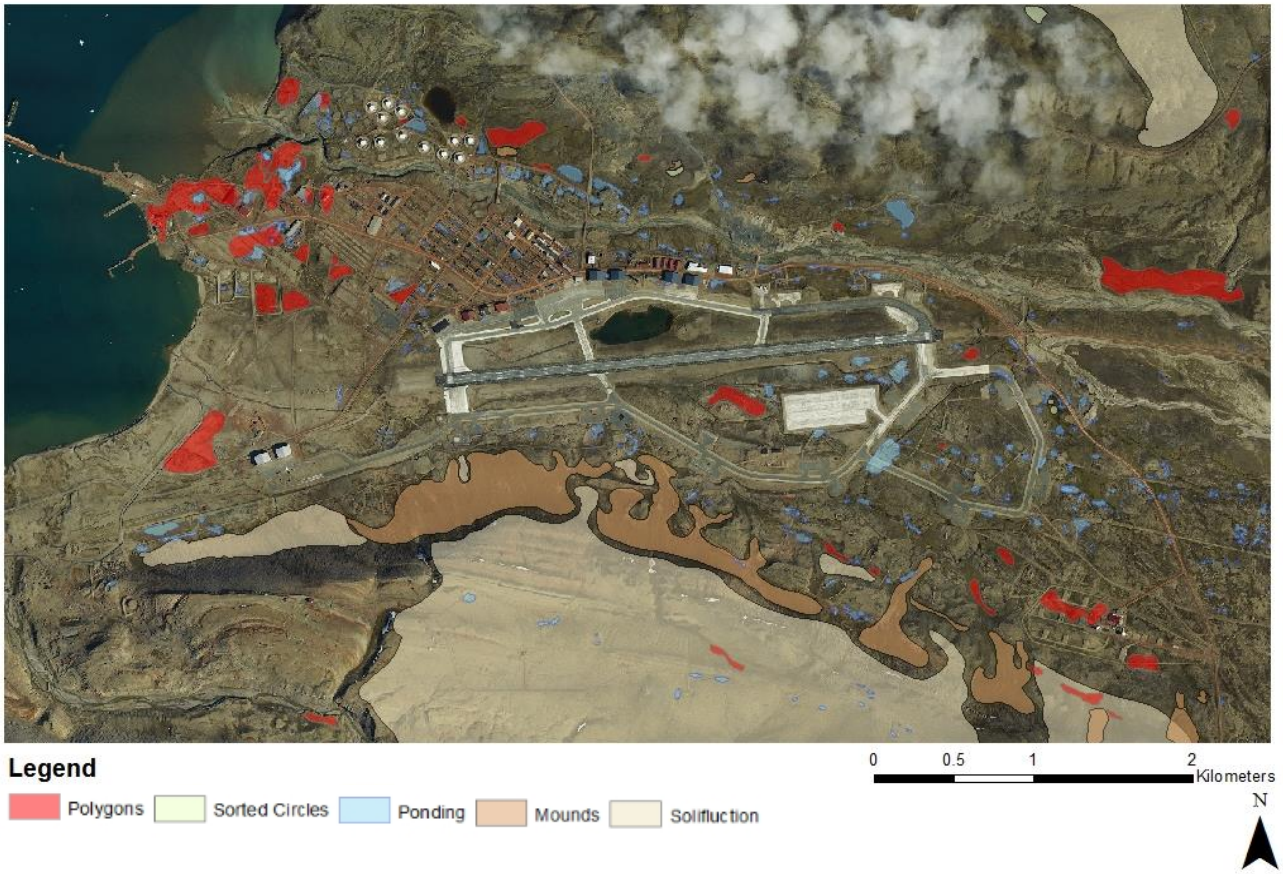

Figure 19. Locations of Permafrost Related Features

Figure 20 provides a partial view of the distribution of specific permafrost-related hazards at Thule Air Base. It represents a snapshot of the hazards present in specific areas in 2018 based on historical photos available from 1952. It is not a complete picture of permafrost hazards for the following reasons: the surface is dynamic due to yearly frost action, many permafrost features are not visible from the surface, much of the surface has been disturbed by human activity, and the historical photos of the virgin surface were unavailable. This is a living map that can inform community planning conversations; however, it must be emphasized that all future work and maintenance require further engineering investigation. Additionally, this map should be expanded and updated periodically to reflect new insights and available data.

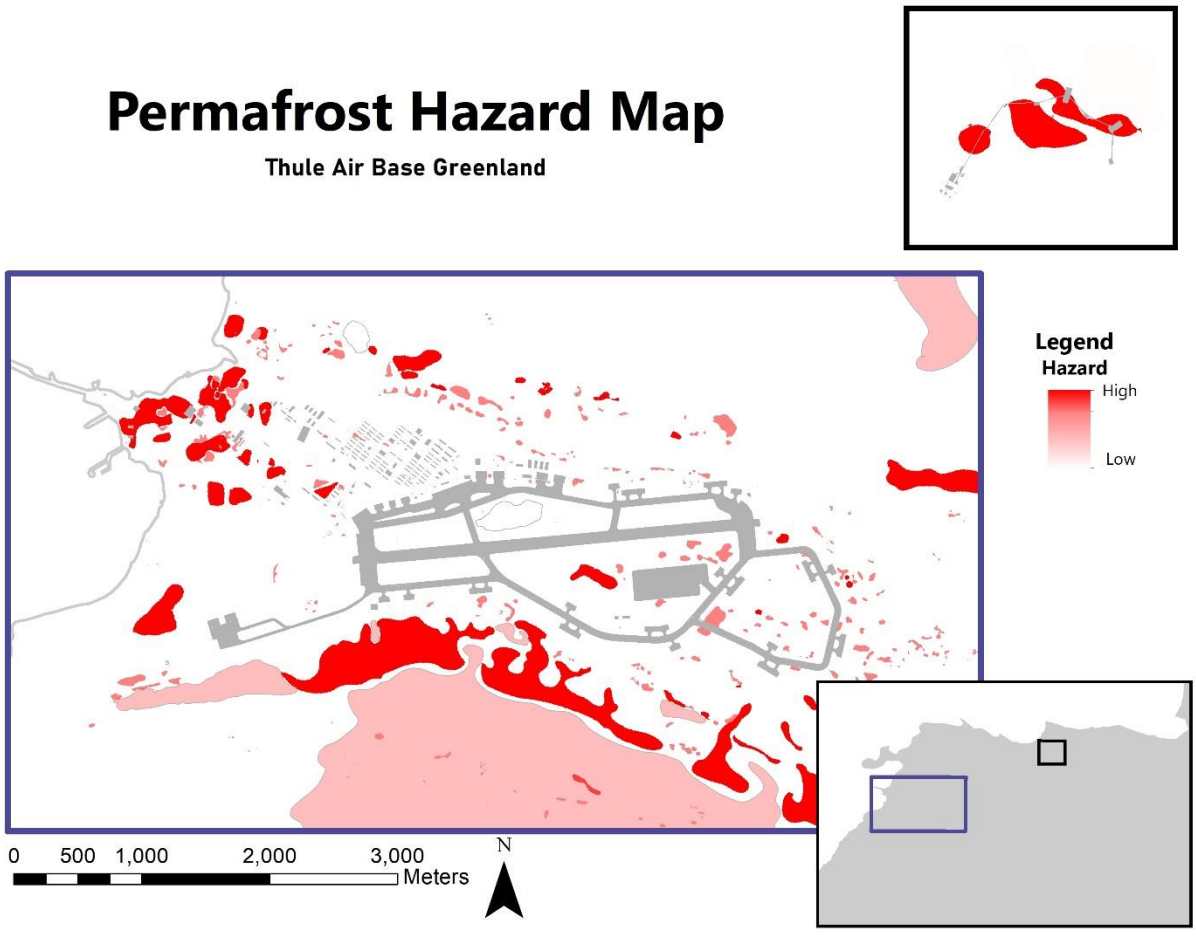

Figure 20. Permafrost Hazard Map Based on Visible Features

The hazard map resulting from the observations of this study suggests that a majority of the concentrated hazards related to permafrost features exist on the southern edge of the data extent and on the west coast of the base around the river delta, but there is a lack of hazards in the main living area of the base and around the airfield. Specific facility reports also facilitate the understanding of the observations and raise further questions. Building 236, the Top of the World Club, is located at the heart of the main living area northwest of the airfield and is currently closed due to severe damage attributed to permafrost decay that resulted from saturation of the ground underneath the facility. Ice features were identified using ground penetrating radar (Bjella, 2016). Although permafrost features are not identified in the hazard map, it is possible that the features were visible before the ground was disturbed. Furthermore, internal leaks and spillage were determined to be the main contributors to the loss of thermal balance and the decay of the permafrost (Bjella, 2016). Polygons are abundantly visible around Building 4002 and its surrounding facilities, which is consistent with historical observation and modern studies of the area (Bjella, 2018). Another area showing polygons directly near facilities is in the southeast corner near the satellite communication areas. These are critical facilities that to this point have no documented reports of serious damage, but they are in close proximity to high-risk features. It is important to continue to maintain the facility's drainage and internal heat sources or risk damage to the foundation. The observations made in this study specifically concerning permafrost features are supported by the field observations from Operation Nanook (Hunt, 1946). Observations of the southern edge of the valley made in 1946 provide details of terraced ground, with ponding at the foot of each terrace. Descriptions of solifluction are also provided (Hunt, 1946). These observations support the occurrence of solifluction and possible ice features in this area.

Drainage Hazards

The results of the ArcMap hydrology analysis revealed many possible drainage hazards near facilities and across the developed areas of the base. Higher accumulation lines shown in Figure 21 are darker than lower accumulation lines and indicate a possibility of saturating the fill beneath a structure or linear construction that may lead to frost heave or an increase in thermal conductivity of the ground, thereby increasing the risk of permafrost thaw as temperatures rise. This map depicts surface flow based on the accumulation from each adjacent cell and does not account for the complex interactions with subsurface drainage and permafrost. This map does, however, present a tool to assess the risks to current facilities from drainage issues.

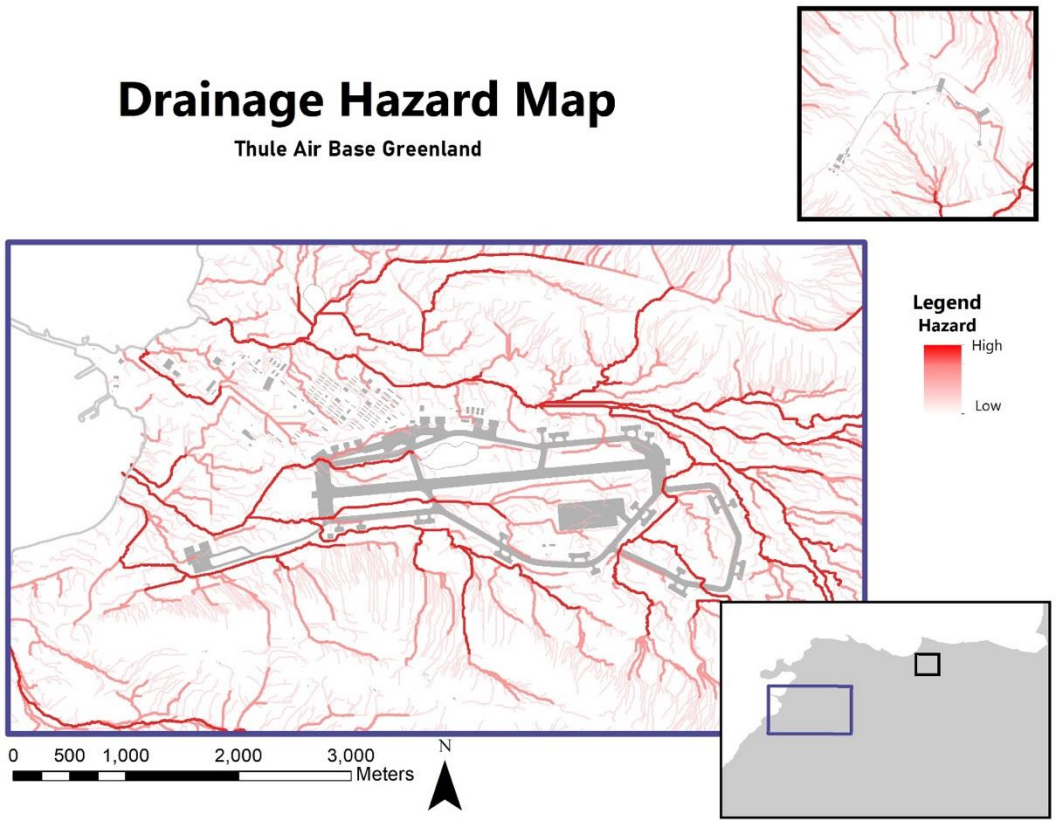

Figure 21. Drainage Accumulation Hazard Map with Accumulation Lines in Shades of Red

Slope Hazards

The results of the slope analysis shown in Figure 22 reveal little threat to the developed areas of the base but do indicate hazards to facilities on the southern edge of the valley and to areas of future development. The view of the Ballistic Missile Early Warning System (BMEWS) site in the top right of the slope hazard map indicates a possible threat of severe damage to facilities if the surface is subject to large movements from permafrost thaw or frost action. Small facilities on the east side of South Mountain face a similar threat. This map is purely based on the slope of the surface and does not take into account the soil classification or other variables affecting slope stability.

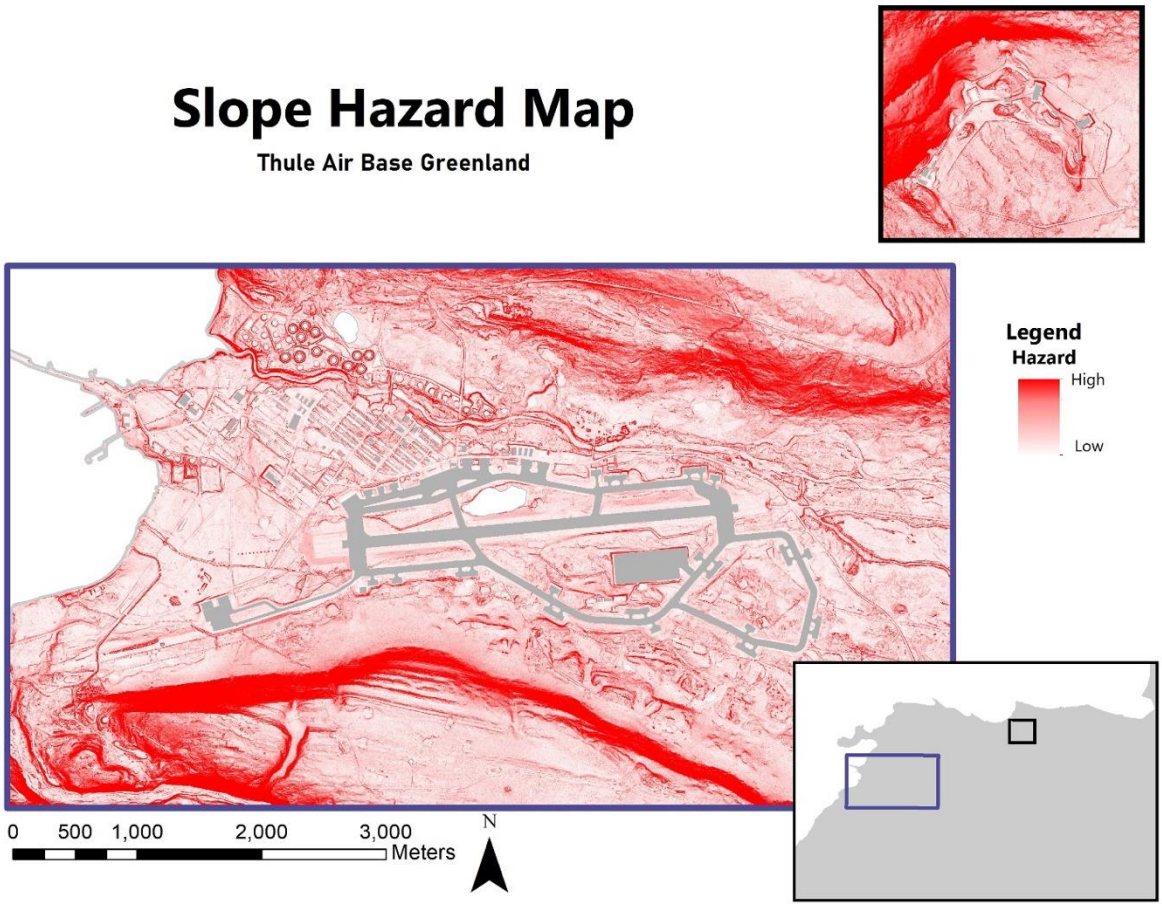

Figure 22. Slope Hazard Map with Steeper Slopes in Darker Red

Cumulative Hazard

Figure 23 represents the summation of hazard scores for each cell from each of the three areas of interest. Each of the three features was given equal weight. Although the southern and western edges of the valley are dominated by higher hazards, the combination of all hazards shows that almost all areas of the base have some degree of hazard. This underscores the need for detailed investigations for future projects. Additionally, the center of the southern runway infield shows a few areas of high hazard that could be surrounded by more hazards that were unidentifiable in this study. Detailed views of areas can be used to inform facility prioritization and investigation planning.

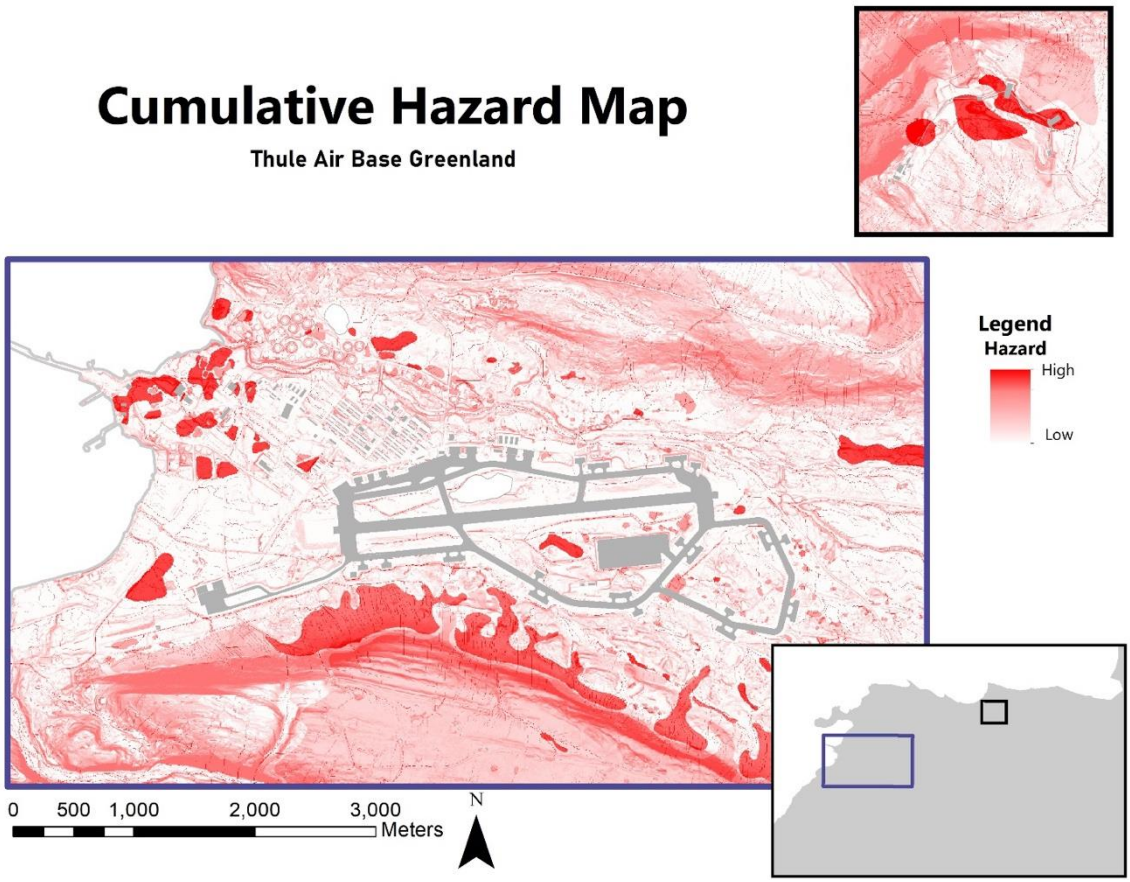

Figure 23. Cumulative Hazard Map Combining Visible Features, Drainage, and Slope

Foundation Condition Assessment

The results of foundation condition assessment of each available facility suggest that there is widespread foundation damage at Thule Air Base. The results of the weighted average of these scores reveal widespread foundation damage at Thule that is often not captured in the Building Condition Index. The average score is 65.5 out of 100 with a standard deviation of 16.6 points. The data from the Vectrus baseline assessments (Baseline) is often drastically different from the foundation condition (A10) and Building Condition Index (BCI) available in the BUILDER system suggesting that either BUILDER may be outdated or thorough inspections were not performed. The scores of this assessment are included in Appendix B.

Foundation Condition and Hazard Location

The final goal of this study was the exploration of the spatial relationship between the distribution of hazards and foundation damage at Thule Air Base. When foundation damage scores were spatially joined to the hazard map, it was unclear from visual inspection of Figure 24 alone if there is a relationship. It does not appear that clusters of darker purple facilities, those with lower condition scores, are found in areas of darker red or higher geotechnical hazard. It is observable that facilities near the coast, at the base of South Mountain, and in the geographically separated BMEWS area are near clusters of higher hazards.

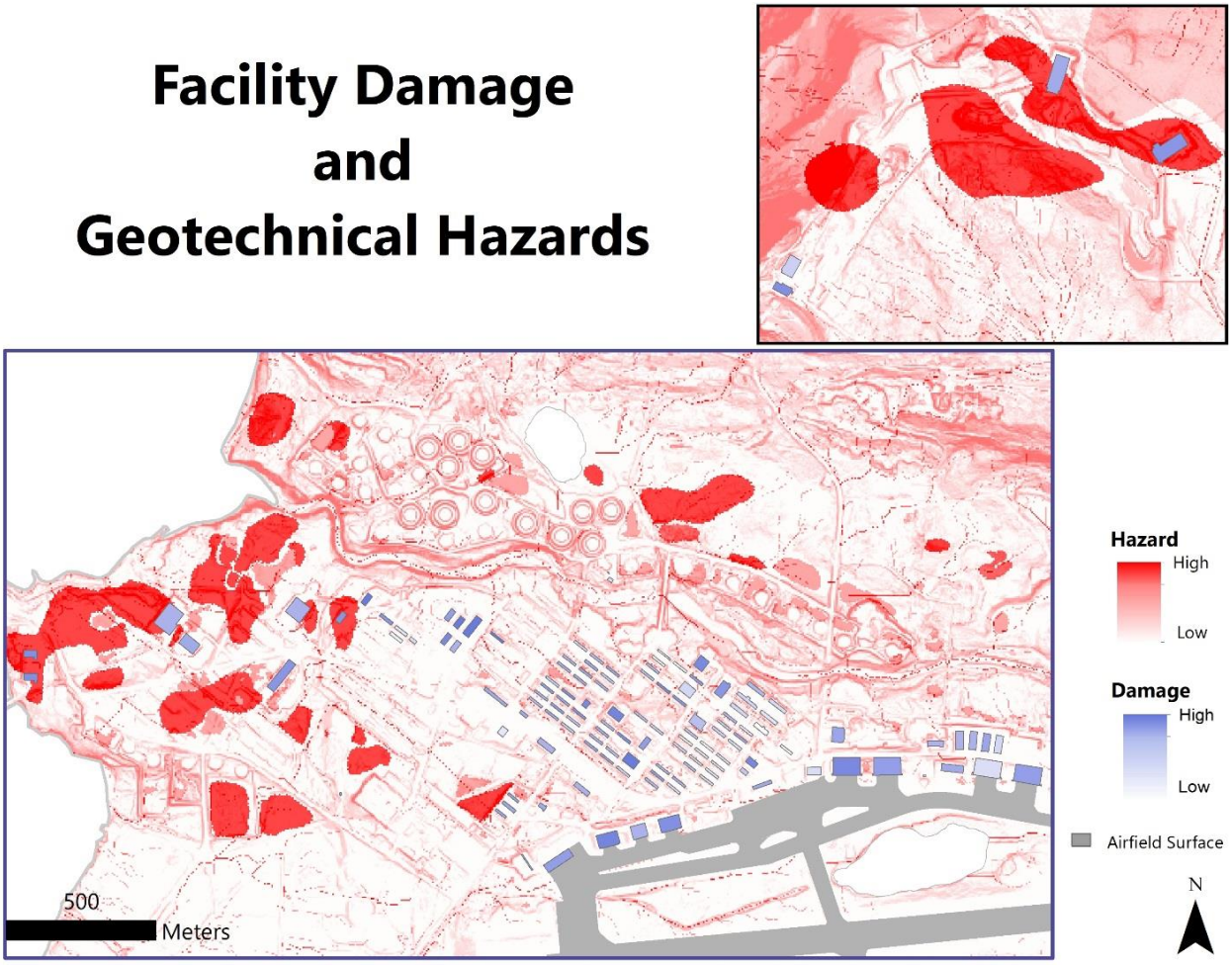

Figure 24. Zoomed View of Cumulative Hazard Map and Facility Damage

Statistical Analysis

Three variables are calculated for this analysis: total hazard, average hazard, and maximum hazard. The total hazard is a summation of all hazard scores within the facility footprint plus 5 meters. The average hazard is the summation divided by the area of the facility footprint. The maximum hazard is the maximum hazard score that exists under the facility footprint plus 5 meters. Descriptive statistics of these metrics are shown in Table 6. The interpretation of these values requires an understanding of the methods used by ArcMap to calculate each score. The total hazard is calculated by summing the value of each cell below the

defined foundation footprint. With each cell having a maximum score ranging from 0 to 16 because the hazards are not mutually exclusive in each cell, a high drainage accumulation, steep slope, and polygon feature would sum to 16 for a single cell. Each of these cells then adds up to give the total score much greater than the 1-4 hazard scale initially defined. The average hazard is then simply the total hazard divided by the area of the foundation, and the maximum hazard is the highest score of a single cell under the facility. These statistics indicate that all facilities face some hazard but that there is a large range across facilities. The top 15 facilities in each category are presented in Table 7 along with the facilities that are on more than two of those lists in Table 8. Table 8 provides context of the facility type to help inform the risk these facilities face. These facilities should be prioritized for future research and investigation. Facilities with high MDI such as the BMEWS site, Hangar, Sewage Treatment, and Dorms pose the greatest consequence of failure if these hazards manifest into physical damage

Table 6. Descriptive Statistics of Facility Hazard Scores

Variable	Mean	Standard Deviation	Minimum	Maximum
Total Hazard	118	196	7.8	1651
Average hazard	1.4	0.7	1	5.4
Max Hazard	2.9	1.3	1.2	7.9

Table 7. 15 Highest Scores for Hazard Statistics

Sum	Avg	Max
4003	4003	4003
4002	4002	4002
1091	1972	974
1090	1971	972
974	974	935
972	972	801
935	935	629
836	801	571
801	571	333
630	343	243
629	342	215
624	333	201
623	331	118
606	117	107
571	115	104

Table 8. Facilities on at Least 2 of the Top 15 Lists in Order of Occurrence

Facility	Name
4003	UEWR (BMEWS)
4002	UEWR (BMEWS)
974	Storage
972	Storage
935	EOC
801	Pavement & Grounds
629	Hangar
571	Base Maintenance
333	Dorm

A statistical analysis of this spatially joined data results in a similarly ambiguous conclusion but suggests that higher hazard areas may have lower foundation condition scores. The results of 20 different iterations are presented in Appendix A. The data was transformed using logarithmic and square root functions and the number of observations in each iteration is based on outliers being removed; the dataset began with 139 observations but had only 125 for the final iterations. Outliers were removed based on being outside 3 standard deviations and 2 standard deviations. Most iterations fail the assumptions necessary to validate linear regression models. In 12 cases, three of four conditions are met: the mean of errors is zero, variance of the errors is constant, and the errors are independent; however, the condition that the errors are normally distributed is not met. An initial analysis would suggest outliers are causing these failures. With the removal of the outliers, the data did meet the assumption normality of errors but still showed autocorrelation of errors, thus suggesting that another relationship may be affecting these variables. Using the total hazard and the square root of the condition score, one iteration performed better than the rest of the OLS Models. This iteration had a p-value of 0.014 but only a very weak fit with a correlation coefficient of 0.048. Based on visual inspection of Figure 25 alone, a higher hazard seems to be related to a lower condition score. This model still exhibited autocorrelation suggesting another relationship may still be present.

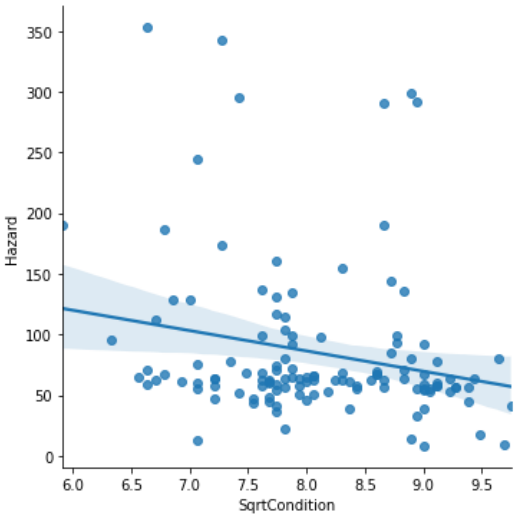

Figure 25. Line of Best Fit for Model Iteration 9 (OLS)

Finally, based on the poor fit of the linear model, a log-based model was explored using statsmodel's logit regression function in Python as shown in Figure 26. This model, resulting in a pseudo r-squared of 0.71, suggests a possible relationship between the two variables, with higher hazard scores resulting in lower condition scores. The pseudo r-squared of a Logistic regression does not indicate the percentage of fit like r-squared in linear regression but still indicates the validity of the model. Based on the visual inspection of plots in Figures 25 and 26, the results of this statistical analysis, and the exploration of outliers, a weak relationship between the variables of hazard and foundation condition may exist, but it is strongly affected by the outliers and the tests of the residuals suggests other relationships may be affecting these variables. The very weak nature of these results warrants further exploration of this relationship and does not provide significant evidence to reject the idea that there is no spatial relationship between these variables.

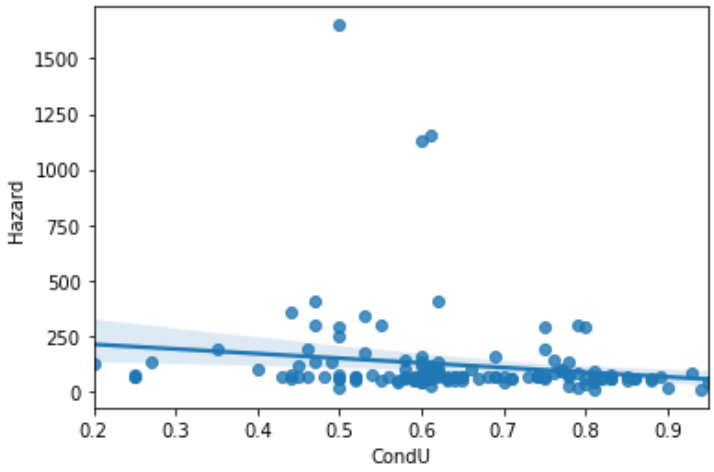

Figure 26. Line of Best Fit for Model Iteration 20 (Logistic)

Summary

The results of a statistical analysis of historical weather data indicate an increase in mean annual air temperature over the last six decades and show that the projected mean temperature estimated for 2030 has already been reached. GIS analysis of aerial photographs and LiDAR data reveals many hazards across the landscape of Thule Air Base; additionally, a weak negative relationship with facility condition is suggested by a statistical analysis. Ultimately, the results validate a threat to the infrastructure and indicate that a spatial relationship may exist but that more research is needed to improve the understanding of a relationship.

Chapter V. Conclusion

The investigation of hazard mapping in the Arctic for infrastructure planning indicates a substantial need for an assessment across Arctic communities. This chapter includes a synopsis of the motivation and rational for investigating this topic followed by a summary of the results in the context of the three research questions developed in Chapter I. The relevance and limitations of the results are then presented to motivate and inform further research and use of the products of this research. Next, suggestions for future research are detailed along with the costs and benefits of continued research. Finally, a summary of the chapter is included.

Motivation

The Arctic is in the midst of a major transition. As a result of retreating sea ice, economic activity has increased along with military activity to protect assets. These transitions to a warmer and less predictable climate, and a more economically and politically active region, are tied to each other, and both have serious implications for Arctic engineering. As the climate continues to warm and ice retreats, human activity continues to increase, which drives the requirement for more infrastructure. The design and maintenance of this infrastructure relies in part on an understanding of climate projections and weather predictions; however, despite warming, the Arctic remains an extreme environment shaped by cryogenic processes. To successfully navigate the future engineering requirements and plan or expand successful settlements, the challenges of the past and present engineering endeavors must be understood. Infrastructure challenges plague the Arctic, and climate change threatens to make them worse, but the distribution of hazards is generally undocumented. This research used available remote sensing data and facility condition data to explore the relationship between the spatial

distribution of geotechnical hazards related to permafrost and the damage to facilities, thus informing maintenance efforts and future community planning.

The focus of this research was a critical Department of Defense (DoD) Arctic base. Thule Air Base in Northwest Greenland is the northernmost DoD installation and houses critical infrastructure that is at the crossroads of the race for Arctic and space dominance. The base is situated on permafrost that reaches to depths of 300 meters and infrastructure across the base has sustained widespread damage from cryogenic action over its 70-year history. As new facilities are planned and budgeting for maintenance is allocated, an understanding of risks is key to future success. Although detailed investigations have been completed on critical facilities that have sustained serious damage, a spatial understanding of the geotechnical hazards across the base and their relationship to recorded facility damage was undocumented prior to this research.

Research Results

This research investigated the climate trends at Thule over the past 70 years, the spatial distribution of hazards, and the relationship between hazards and facility damage. The analysis of weather data and its comparison to climate projections presents a clear picture of future serious risk to Thule Air Base due to warming. The past two decades have seen a substantial increase in Mean Annual Air Temperature (MAAT) that threatens the stability of permafrost and reduces the design life of facilities. Records indicate that Thule has already surpassed the 2030 projections for MAAT, and the base continues to experience record events. Although limited precipitation data is available, a pattern of extreme swings is apparent, and extreme rainfall events combined with poor drainage have been the direct cause of serious damage on base.

These observations signal a need for updated design criteria and a closer look at the precipitation projections for the base.

Using photogrammetry and Geographic Information System (GIS) software, the location of visible features created by cryogenic processes, surface hydrology, and slope were mapped. These identified features were scored to create a geotechnical hazard map for Thule Air Base. The results of this process indicated widespread hazards across the base and concentrated high hazard areas along the coast and southern edge of the valley. When compared to facility damage scores, only a very weak positive relationship between hazards and facility damage is present; however, the statistical analysis suggests that other relationships may be at play between these and other variables. Despite these weak statistical results, the hazard map and damage assessments separately shed light on the risks to infrastructure and the current state of infrastructure at Thule Air Base. The study of aerial photography and of Light Detection and Ranging (LiDAR) data suggest the existence of serious threats to the health of the infrastructure and the risk to future infrastructure from permafrost and drainage accumulation. The maps developed in this research provide a tool for planners to assess the risk of future construction sites to cryogenic processes and to understand the maintenance priorities of current facilities. Regardless of the relationship between facility score and hazard, those facilities located on or near visible permafrost features, drainage accumulation areasr, or slopes are at risk of failure and require attention from engineers. Additionally, the assessment of available data and reports on facility condition indicate widespread foundation damage across the base related to settlement and drainage issues that support this need. This information informs the decisions of facility planners and engineers as they plan new projects and maintain the base.

Relevance

The results of this research provide a communication tool for planners and engineers in discussion with decision-makers on the future of Thule Air Base and the need for maintenance or divesting of a facility in the short-term as well as long-term. The results provide a model for other DoD Arctic bases, or any entity on hazardous landscapes, to assess and communicate the risks to better plan the location and requirements of future facilities. The map produced for Thule Air Base, for example, identifies a high concentration of hazards on the coast, which indicates a need for serious investments in the investigation of the geotechnical properties of the area or avoidance of the area all together if there is a low tolerance for risk or the budget does not allow for extensive earthwork. The map additionally identifies many points of drainage intersection with facilities, which increases the risk of damage from water infiltration of the fill and subsequent heave and/or shrinkage. This signals the need for a widespread monitoring and maintenance of the drainage around facilities, as well as the need for more robust drainage measures for new facilities. This research is also relevant due to the timing of increased activity in space and the Arctic. With the development of the United States Space Force under the Department of the Air Force and continued competition in space, the assets housed in the Arctic are of great importance to the DoD and future development of the base is inevitable. Additionally, with the political importance of the Arctic growing as resources become available, the stability of the region relies on the stability of the United States bases and their infrastructure.

Limitations

The relevance of these results is limited by four major factors: the nature of hazard maps and foundation design, the availability of data and processing power, the dynamic nature of

Arctic landscapes, and the expertise of the researcher. Facility design and construction require in-depth geotechnical investigations in order to achieve economically feasible products and ensure the safety of the end users. The hazards identified in this study do not represent the exact subsurface conditions for use in the determination of foundation design. Instead, the hazard maps presented in this research should be considered living maps that suggest (1) the risk to existing and future facilities and (2) the potential for costly geotechnical investigations and earthwork. The hazard map fits into a similar type of tool as the installation development plan (IDP) used by Air Force planners and should even be considered an important part of future IDPs.

The next limitation is data and processing power availability. Permafrost is in a fragile state of thermal balance that is easily disrupted by human activity, thereby shifting the active layer down and resulting in a loss of visible surface features (Muller, 1947). This fact makes high resolution aerial photographs of untouched landscapes invaluable to understanding the subsurface features of a permafrost landscape. With limited photos of this natural landscape, parts of the hazard map are missing this historical aspect and do not capture the full extent of possible hazards to the existing facilities. Additionally, missing rainfall and river level data prevent the analysis of the additional threats from flooding. While much data remained unattainable, the size of the existing data posed a large challenge for processing. With over 100 gigabytes of remote sensing data available for this small area and some individual files exceeding 1 gigabyte in size, a reduction in resolution was required for the successful analysis of the data in GIS software. Even with a reduction in resolution, the hazard map included over two million data points, which took hours of processing using the tools in ArcMap. This processing lag prevents the iteration of the mapping and analysis process. Based on the availability of

resources at the time of the research, processing power became a large limitation in the final product.

Finally, the relevance of a hazard map is time dependent because of the dynamic nature of Arctic landscapes. Even without increasing temperatures and a possible increase in precipitation, the Arctic landscape is already under constant change from the hydrologic cycle (Woo, 2014). As water freezes and thaws, and flows from the ice cap to the ocean, sediment is transformed and transported and thus the landscape is also transformed. Therefore, to fully understand hazards, these maps require a temporal component to help understand the types and rates of change occurring to the landscape as these factors will play a role in the short-term and long-term risk to infrastructure.

A major challenge of permafrost research is that it is at the crossroads of many disciplines. This research in particular derives concepts from geotechnical engineering, foundation engineering, hydrology, thermodynamics, geology, photogrammetry, computer science, and others. Without being an expert in any of these disciplines, the outcomes of this research are heavily influenced by the correct application of the principles of these disciplines. In particular, a certification for a photogrammetric specialist exists to validate the experience of an individual in studying and deriving data from photographs. Future maps would benefit greatly from the review of experts in these fields.

Future Research

The results of this research highlight opportunities for future research to further develop an understanding of Arctic hazards. Understanding local weather trends in order to develop detailed engineering criteria is the first step in successfully adapting to the changes ahead. To

develop these criteria though, more detailed precipitation data is needed. This data will further inform the understanding of drainage and flooding hazards. Exploring the trend of freeze-thaw cycles, which serves as the driver of cryogenic processes and the direct cause of the heave of saturated fill, can help inform decisions related to the risk of facility damage from drainage issues. Improving climate projections can also play a role in adapting to changes. The Air Force weather squadron currently uses 10 years of data to inform projections, but with more data available projections may be able to be improved. These projections may indicate more or less risk of permafrost decay and icecap runoff at Thule.

Additional study of the hazards at Thule and other Arctic bases is also prudent in the preparation for future investments. Other hazards such as soil classification, water table depth, and coastal erosion can be included in future hazard maps to better encompass the full range of threats to the base infrastructure. One major threat that has the potential for serious risk is flooding. Currently, there is no flood plain mapping at Thule, even though facilities are in very close proximity to the major river in the valley. Some river depth data exists but was unavailable for this study; since monitoring of the river has ceased, a return to monitoring would provide a huge benefit to the security of the base. Melting of the icecap, rainfall, and snowmelt all play a part in the river height and flood potential, and the risks are currently undocumented related to these topics.

Another opportunity for continued research is the study of historical aerial photos located at the National Archives in College Park, Maryland. As mentioned in the limitations of this study, photos of undisturbed ground are key to understanding current threats that may exist directly underneath facilities. As part of this research, these photos were located; however, they could not be accessed due to the COVID environment. Clues to the existence of these photos are

provided by reports about the planning for Operation Blue Jay, the secret construction of Thule Air Base.

One specific aerial photo, shown in Figure 27, includes reference to the mission for which the photo was collected. When searching this string of information, the 311th Reconnaissance Wing is included in the results. During World War II and the Cold War, the 311th Reconnaissance Wing conducted data collection missions over Greenland (Cahill, 2014); this supports the hypothesis that more of these photos exist. The National Archives online databased was searched using the latitude and longitude of Thule Air Base and a result included the location of Thule under Record Group 373 Series: Overlay Indexes for Aerial Photography of the Defense Intelligence Agency, 1935 – 1971. As the Army Map service became the Defense Intelligence Agency, this record seemed to point in the right direction. Examination of the collection of records revealed the exact label found on the picture from the report. The tag number was searched in the Archives photo storage records and found to be in cold storage in Kansas. These photos are critical to future research and even operational success; although global factors prevented the acquisition of these photos, they hopefully have been scanned.

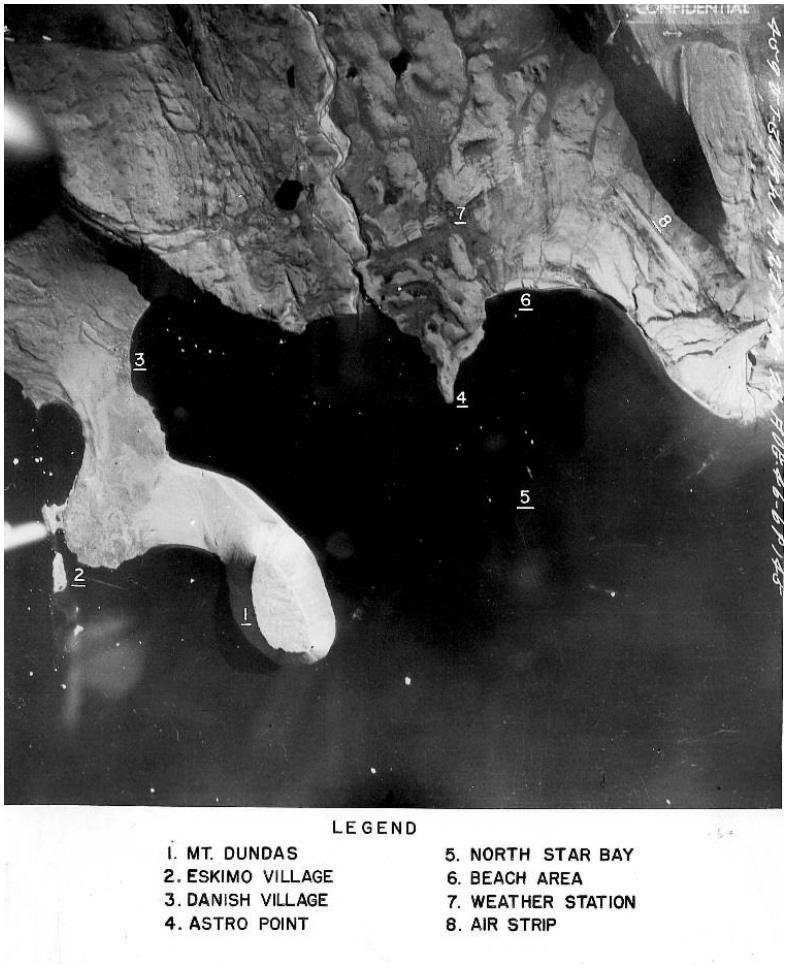

Figure 27. Aerial Photograph from Operation Blue Jay Report

The results of this study naturally lend themselves to follow-on case studies. During the completion of this research, a four-day rain event caused severe damage on the airfield, as shown in Figure 28. Severe depressions appeared in the shoulder almost overnight which posed serious risks to the runway from loss of lateral confinement. Although cracks were sealed and fill was placed in the larger fissures before the freeze in September, this continues to pose a serious risk as the shoulders remain uninsulated and pockets of massive ice have been found in the area. With historical aerial photographs to identify visible permafrost features, a relationship can be established between the excavated massive ice and segregated ice, shown at the top of Figure 28,

and the surface morphology to predict high risk areas of the shoulder or runway. A study of pavements around the base, including the runway, using available PAVER data inspection reports and field work could follow a similar methodology to the study of foundations. Additional studies should also be completed on critical facilities in proximity to hazards such as the radar and satellite communication equipment.

Figure 28. Severe Airfield Damage and Nearby Massive Ice

This study also demonstrated the utility of detailed foundation condition reports. Although Vectrus completed these studies at the start of their base maintenance contract in 2017 to reduce liability for existing issues left by the previous contractor, this data was crucial to understanding the state of foundations across the base and provided the detail required to create a credible foundation condition score. More baseline reports such as this would benefit the Air Force greatly.

Costs and Benefits of Research

With the strategic importance of the base and its infrastructure established by the 2020 Arctic Strategy, the question remains, "What is the required future investment in the base, and what is the cost of ignoring hazard risks?" The plant replacement value of the structures at Thule Air Base alone is 1.6 billion U.S. dollars, with real property on the base valued at 4.2 billion dollars and 10 years of maintenance costing 1 billion dollars (USA Spending, 2005). With the possibility of billions more in modernization and expansion as a result of the DoD Arctic Strategy, the investigation of engineering challenges remains paramount, not only for the success of the mission but also to the fiscal stewardship of the U.S. government. The survey conducted to collect high resolution LiDAR and imagery in 2018 cost around 5 million dollars and produced an abundance of data for use in identifying hazards (USA Spending, 2018). To fully understand the rate of decay of permafrost at Thule, the cost of data collection is well worth the possible cost of replacing facilities, especially when foundation damage is serious in nature.

Summary

The results of this study indicate serious risk to the infrastructure at Thule Air Base. Widespread foundation issues, warming temperatures, extreme precipitation patterns, abundant permafrost features, and drainage and slope stability hazards present a threat to the longevity of the base and the economic feasibility of future development of the base to support growing missions. The hazard maps created in this study provide a tool for community planners to communicate risk to decision-makers and inform future areas of study. The weak relationship established between hazards and foundation damage guides the way for future research to expand the data, explore more relationships, and involve experts in the analysis of threats. To be

successful in the Arctic, serious attention must be paid to the geotechnical investigation and community planning efforts of future facilities in support of critical missions. As the Air Force continues to find ways to adapt to climate change, it is prudent to work with the forces of nature and understand the lessons of the past as we seek to be resilient to the continual changes that nature undergoes.

References

AFCEL. (1955). "Report of Thaw Penetration and Subsidence, Runway and Taxiway Sections, Thule Air Force Base" *Arctic Construction and Frost Effects Laboratory*. U.S. Army Cold Regions Research and Engineering Laboratory, CRREL TR-54.

AMAP. (2019). "AMAP Climate Change Update 2019: An Update to Key Findings of Snow, Water, Ice and Permafrost in the Arctic (SWIPA) 2017*". Arctic Monitoring and Assessment Programme (AMAP)*, Oslo, Norway. 12 pp.

AMAP (2017). "Snow, Water, Ice and Permafrost. Summary for Policy-makers". *Arctic Monitoring and Assessment Programme (AMAP)*, Oslo, Norway. 20 pp

Andersland, O. B., & Ladanyi, B. (1994). *An Introduction to Frozen Ground Engineering*. https://doi.org/10-1007/978-1-4757-2290-1

Arenson, Lukas U., William Colgan, and Hans Peter Marshall. (2015). "Physical, Thermal, and Mechanical Properties of Snow, Ice, and Permafrost." *Snow and Ice-Related Hazards, Risks and Disasters, eds*. John F. Shroder, Wilfried Haeberli, and Colin Whiteman. Boston: Academic Press, 35–75. http://www.sciencedirect.com/science/article/pii/B9780123948496000020 (Accessed 5 August 2020)

Army Map Service. (1952). *AMS C501 Greenland 1:250,000 Topographic Series.* Retrieved December 2, 2020 from https://maps.apps.pgc.umn.edu/id/363

Agard John, Schipper, E. Lisa F. (2014) "IPCC WGII AR5 Glossary". 1–51. <https://www.ipcc.ch/site/assets/uploads/2018/02/WGIIAR5AnnexII_FINAL.pdf > (Accessed 12 December 2020)

Benninghoff, William S. (1953). "Use of Aerial Photographs for Terrain Interpretation Based On Field Mapping". United States Geological Survey <http://www.asprs.org/wp-content/uploads/pers/1953journal/jun/1953_jun_487-490.pdf>(Accessed 3 August 2020)

Benkert, B., Kennedy, K., Fortier, D., Lewkowicz, A., Roy, L.-P., De Grandpré, I., Grandmont, K., Drukis, S., Light, E., and Williams, T. (2016). "Old Crow landscape hazards: Geoscience mapping for climate change adaptation planning".

Bevis, M., Harig, C., Khan, S. A., Brown, A., Simons, F. J., Willis, M., Fettweis, X., Broeke, M. R. van den, Madsen, F. B., Kendrick, E., Caccamise, D. J., Dam, T. van, Knudsen, P., and Nylen, T. (2019). "Accelerating changes in ice mass within Greenland, and the ice sheet's sensitivity to atmospheric forcing". *Proceedings of the National Academy of Sciences, National Academy of Sciences*, 116(6), 1934–1939.

Bintanja, R., Andry, O. (2017). "Towards a rain-dominated Arctic". Nature Climate Change 7, 263–267. https://doi.org/10.1038/nclimate3240

Bjella, K. (2019). “Thule Air Base Trip Report November 2019 B/4002, B/1391, B/4016”. ERDC-CRREL, Cold Regions Research and Engineering Laboratory (CRREL), Hanover, USA.

Bjella, K. (2018). “Thule Air Base Building 4002 Pedestal and Tunnel Investigation”. Cold Regions Research and Engineering Laboratory (CRREL), Hanover, USA.

Bjella, K. (2016). “Thule Air Base Building 236 – Settlement and Permafrost Investigation Draft”. Cold Regions Research and Engineering Laboratory (CRREL), Hanover, USA.

Bjella, K. (2015) “Geotechnical Study and Foundation Structural Design, Next Generation Ionosonde (NEXION) Installation, Thule Air Base, Greenland”. ERDC/CRREL Letter Report LR 15-13. Cold Regions Research and Engineering Laboratory (CRREL), Hanover, USA.

Bjella, K. (2010) “Air-Ducted Hangar Foundations at Thule, Greenland”. Cold Regions Research and Engineering Laboratory, Ft. Wainwright, Alaska, USA

Black, R. F. (1976). *Features Indicative of Permafrost*. Annual Review of Earth and Planetary Sciences, 4(1), 75–94. <https://www.annualreviews.org/doi/abs/10.1146/annurev.ea.04.050176.000451>(Accessed 5 August 2020)

Boike, Julia, and Kenji Yoshikawa. (2003). “Mapping of Periglacial Geomorphology Using Kite/Balloon Aerial Photography”. *Permafrost and Periglacial Processes* 14(1): 81–85.

Brown, Jerry, and Vladimir E. Romanovsky. (2008). “Report from the International Permafrost Association: State of Permafrost in the First Decade of the 21st Century”. *Permafrost and Periglacial Processes* 19(2): 255–60.

Cahill, William. (2014). “Reconnaissance on a Global Scale: SAC Reconnaissance of the 1950s”. *Air Power History* 61(1): 14–29.

Carmona, A. M., and G. Poveda. (2014). “Detection of long-term trends in monthly hydro-climatic series of Colombia through empirical mode decomposition”. *Climatic Change*, 123, 301–313, https://doi.org/10.1007/s10584-013-1046-3.

Ching, Jianye, and Kok-Kwang Phoon. (2012) “Value of Geotechnical Site Investigation in Reliability-Based Design.” *Advances in Structural Engineering*, vol. 15, no. 11, SAGE Publications Ltd STM, Nov. 2012, pp. 1935–45. *SAGE Journals*, doi:10.1260/1369-4332.15.11.1935.

Coduto, D. P., Kitch, W. A., & Man-Chu Ronald Yeung. (2016). *Foundation design: principles and practices*. Pearson.

Corte, A.E. (1962). “Relationship Between Four Ground Patterns, Structure of the Active Layer, and Type and Distribution of Ice in the Permafrost”. Cold Regions Research and Engineering Laboratory (CRREL), Hanover, NH. CRREL Research Report 88.

Cova, TJ. (1999). “GIS in Emergency Management”. *Geographic Information Systems Principles and Technical Application Management* 845–858.

Daanen, R. P., Ingeman-Nielsen, T., Marchenko, S. S., Romanovsky, V. E., Foged, N., Stendel, M., Christensen, J. H., and Hornbech Svendsen, K. (2011). “Permafrost degradation risk zone assessment using simulation models”. *The Cryosphere*, 5(4), 1043–1056.

Davis, T. N. (2001). “Permafrost: A guide to frozen ground in transition”. Fairbanks, AK: Univ. of Alaska Press.

Davies, W., D. Krinsley and A. Nicol. (1963). “Geology of the North Star Bugt Area, Northwest Greenland”. *Meddelelser om Groenland*, 162(12).

DoD. (2020). “2020 Department of Defense Arctic Strategy”. <https://www.af.mil/Portals/1/documents/2020SAF/July/ArcticStrategy.pdf>(Accessed 31 July 2020)

Dod, K. (n.d.). “Chapter XIV Securing the Norther Bastions: Greenland and Iceland*”*. *Overseas Military Operations of the Corps of Engineers, 1945 - 1970.*

Doré, Guy, Niu, Fujun, Brooks, Heather. (2016). “Adaptation Methods for Transportation Infrastructure Built on Degrading Permafrost”. *Permafrost and Periglacial Processes* 27(4): 352–64.

Douglas, T. A., Bjella, K., and Campbell, S. W. (2013). “What’s down below? Current and potential future applications of geophysical techniques to identify subsurface permafrost conditions”. *AGU Fall Meeting Abstracts*, 53, C53C-01.

ESRI. (2020). “Overview of georeferencing”. *Imagery and raster in ArcGIS Pro*. <https://pro.arcgis.com/en/proapp/latest/help/data/imagery/overview-of-georeferencing.htm>(Accessed 5 November 2020)

Flynn, M., Ford, J. D., Labbé, J., Schrott, L., and Tagalik, S. (2019). “Evaluating the effectiveness of hazard mapping as climate change adaptation for community planning in degrading permafrost terrain”. *Sustainability Science*, 14(4), 1041–1056.

Hansen, E. (1994). “40 years of foundation collapse in permafrost Thule Air Base, Greenland. Case history 1953 -1993. Including repair project 1992 –1993”. *In proceedings of Polartech ’94*. Lulea, Sweden.

Hjort, J., Karjalainen, O., Aalto, J., Westermann, S., Romanovsky, V. E., Nelson, F. E., Etzelmüller, B., and Luoto, M. (2018). “Degrading permafrost puts Arctic infrastructure at risk by mid-century”. *Nature Communications*, 9.

Hopkins, D. M., and Karlstrom, T. N. V. (n.d.). “Permafrost and Ground Water in Alaska”. 69. <https://pubs.usgs.gov/pp/0264f/report.pdf> (Accessed 1 August 2020)

Howard, Roger. (2009). “The Arctic Gold Rush: The New Race for Tomorrow’s Natural Resources”. Bloomsbury Publishing.

Hunt, Ralph W. (1946) “Report of Operation Nanook”. *Fort Belvoir, Va: Arctic Research Section, the Engineer School*. Print.

IPCC. (2019) “Summary for Policymakers”. *IPCC Special Report on the Ocean and Cryosphere in a Changing Climate* [H.-O. Pörtner, D.C. Roberts, V. Masson-Delmotte, P. Zhai, M. Tignor, E. Poloczanska, K. Mintenbeck, A. Alegría, M. Nicolai, A. Okem, J. Petzold, B. Rama, N.M. Weyer (eds.)]. In press.

International Permafrost Assosiation. (1997) “IPA Permafrost Map”. <https://ipa.arcticportal.org/products/gtn-p/ipa-permafrost-map> (Accessed 5 September 2020)

Jorgenson, M. Torre., 2010. “Resilience and Vulnerability of Permafrost to Climate”. *Canadian Journal of Forest Research* 40(7): 1219–36.

Käpyla, Juha, and Harri Mikkola. (n.d.). “Arctic Conflict Potential: Towards an Extra-Arctic Perspective”. *The Finnish Institute of International Affairs.* <https://www.files.ethz.ch/isn/189844/wp85.pdf> (Accessed 14 August 2020)

Karjalainen, O., Aalto, J., Luoto, M., Westermann, S., Romanovsky, V. E., Nelson, F. E., Etzelmüller, B., and Hjort, J. (2019). “Circumpolar permafrost maps and geohazard indices for near-future infrastructure risk assessments”. *Scientific Data, Nature Publishing Group*, 6(1), 190037.

Karl, Thomas R, Knight, Richard W. and Plummer, Neil. (1995). “Trends in High-Frequency Climate Variability in the Twentieth Century”. *Nature* 377(6546): 217–20.

Kopec, Ben G., Xiahong Feng, Fred A. Michel, and Eric S. Posmentier. (2016). “Influence of Sea Ice on Arctic Precipitation”. *Proceedings of the National Academy of Sciences* 113(1): 46–51.

Kronik, Y. A. (2001). “Accident rate and safety of natural–anthropogenic systems in the permafrost zone”. *In Proceedings of the Second Conference of Russian Geocryologists*, 4: 138–146.

Lau, K.-M., and H. Weng. (1995). “Climate signal detection using wavelet transform: How to make a time series sing”. *Bull. Amer. Meteor. Soc.*, 76, 2391–2402, https://doi.org/10.1175/1520-0477(1995)076<2391:CSDUWT>2.0.CO;2.

Lai, Yuchuan, and David A. Dzombak. (2019). “Use of Historical Data to Assess Regional Climate Change”. *Journal of Climate* 32(14): 4299–4320. <https://journals.ametsoc.org/jcli/article/32/14/4299/344026/Use-of-Historical-Data-to-Assess-Regional-Climate>(Accesssed 21 September 2020)

Linell, K. A. and Lobacz, E. F., 1980. "Design and construction of foundations in areas of deep seasonal frost and permafrost*"*. U. S. Army, Cold Regions Research and Engineering Laboratory, Special Report 80-34.

Martel, Jean-Luc, Alain Mailhot, François Brissette, and Daniel Caya. (2018). "Role of Natural Climate Variability in the Detection of Anthropogenic Climate Change Signal for Mean and Extreme Precipitation at Local and Regional Scales". *Journal of Climate* 31(11): 4241–63.

Martin, Philip D., Jennifer L. Jenkins, F. Jeffrey Adams, M. Torre Jorgenson, Angela C. Matz, David C. Payer, Patricia E. Reynolds, Amy C. Tidwell, and James R. Zelenak. (2009). "Wildlife Response to Environmental Arctic Change: Predicting Future Habitats of Arctic Alaska. Report of the Wildlife Response to Environmental Arctic Change (WildREACH)". *Predicting Future Habitats of Arctic Alaska Workshop*, 17-18 November 2008. Fairbanks, Alaska: U.S. Fish and Wildlife Service. 138 pages.

Martin-Nielsen, J. (2012). "The other cold war: the United States and Greenland's ice sheet environment 1948–1966*"*. *Journal of Historical Geography*, 38(1), 69–80.

McAnerney, J.M. (1968). "Investigation of Subsurface Drainage at the BMEWS Facility, Thule, Greenland". *Special Report SR-111*. Cold Regions Research and Engineering Laboratory, Hanover, NH, USA.

Melillo, J. M., T. T. C. Richmond, and G. W. Yohe. (2014). "Climate Change Impacts in the United States: The Third National Climate Assessment". *U.S. Global Change Research Program*, 841 pp.

Muller, S. W. (1947). "Permafrost or Permanently Frozen Ground and Related Engineering Problems". *Washington, DC: Off. Chief Engineers, US Army*. 231 pp. (Lithoprinted 1947. Ann Arbor, Mich: Edwards Bros.)

Northern Climate ExChange. (2016). "Hazard Mapping in the North: A review of approaches for key hazard types". *Yukon Research Centre*, Yukon College.

Obu, Jaroslav et al. 2019. *Northern Hemisphere Permafrost Map Based on TTOP Modelling for 2000–2016 at 1 km2 Scale*. Earth-Science Reviews 193: 299–316.

Pick, Lewis A. (1953). "The Story of BLUE JAY". *The Military Engineer* 45 (July–Aug. 1953): 278

Rasmussen, K. (n.d.). "Greenland by the Polar Sea; the story of the Thule expedition from Melville bay to Cape Morris Jesup". F.A. Stokes, New York :, 1–476.

Romanovsky, Vladimir E. (2007) "Frozen Ground. Global Outlook for Ice & Snow". *Division of Early Warning and Assessment (DEWA), United Nations Environmental Programme*, pp. 181–200.

Rudy, A. C. A., Lamoureux, S. F., Treitz, P., and Collingwood, A. (2013). "Identifying permafrost slope disturbance using multi-temporal optical satellite images and change detection techniques". *Cold Regions Science and Technology*, 88, 37–49.

Saunders, James. (1851) "Proceedings of HMS North Star". *Accounts and Papers of the House of Commons 4 Feb-8 Aug. 1851*

Schmertmann, J. H., and Taylor, R. S. (1965). "Quantitative data from a patterned ground site over permafrost*"*. Technical Report, Cold Regions Research and Engineering Laboratory (U.S.).

Seager, T. P., Clark, S. S., Eisenberg, D. A., Thomas, J. E., Hinrichs, M. M., Kofron, R., Jensen, C. N., McBurnett, L. R., Snell, M., and Alderson, D. L. (2017). "Redesigning Resilient Infrastructure Research*". Resilience and Risk, NATO Science for Peace and Security Series C: Environmental Security, I. Linkov and J. M. Palma-Oliveira, eds*., Springer Netherlands, Dordrecht, 81–119.

Shea, Niel., 2019. "A New Cold War Brews as Arctic Ice Melts". *National Geographic*. <https://www.nationalgeographic.com/environment/2018/10/new-cold-war-brews-as-arctic-ice-melts/> (Accessed 14 August 2020).

Shur, Y., and Goering, D. J. (2009). "Climate Change and Foundations of Buildings in Permafrost Regions*". Permafrost Soils, Soil Biology, R. Margesin, ed.*, Springer, Berlin, Heidelberg, 251–260.

Smith, M. W., and D. W. Riseborough. (2002). "Climate and the Limits of Permafrost: A Zonal Analysis". *Permafrost and Periglacial Processes* 13(1): 1–15.

Streletskiy, D. A., Shiklomanov, N. I., and Nelson, F. E. (2012). "Permafrost, Infrastructure, and Climate Change: A GIS-Based Landscape Approach to Geotechnical Modeling". *Arctic, Antarctic, and Alpine Research*, Taylor & Francis, 44(3), 368–380.

Tarolli P, Cavalli M., 2013. "Geographic Information Systems (GIS) and Natural Hazards*". Encyclopedia of Natural Hazards* 378–385.

Tobiasson, W. and Lowry III, J., 1970. "Hangar Floor Settlements at Thule Air Base, Greenland". *US. Air Force Technical Report No. AFWL-TR-69-122*. Air Force Weapons Laboratory, Kirtland Air Force Base, New Mexico.

Thoman, R. L., Richter-Menge, J., Druckenmiller, M. L. (2020). "National Oceanic and Atmospheric Administration. Arctic Report Card 2020: Executive Summary". https://doi.org/10.25923/MN5P-T549

Thule Air Base Maintenance Contract. (2017). "Contract Number FA2523-15-C-0001". Provided by Thule Air Base Civil Engineer Flight

USACE. (1964). "1963 BMEWS Subsurface Investigation". US Army Corps of Engineers District, New York Corps of Engineers.

USA Spending. (2018). “Spending by Prime Award: Woolpert”. <https://www.usaspending.gov/search/9ce24748670cdc88b03a033af1172d70> (Accessed 23 December 2020)

USA Spending. (2005). “Spending by Prime Award: Greenland Contractors”. <https://www.usaspending.gov/search/9651ca1039209034a714769575a219f4> (Accessed 23 December 2020)

Walsh, John E. (2008). *Climate of the Arctic Marine Environment*. Ecological Applications 18(sp2): S3–22.

Washburn, A. L. (1973). “Periglacial Processes and Environments”. New York: st. Martin's Press, 318 pp.

Wei, M., Guodong, C., and Qingbai, W. (2009). “Construction on permafrost foundations: Lessons learned from the Qinghai–Tibet railroad”. *Cold Regions Science and Technology*, 59(1), 3–11.

Woo, Ming-ko. (2012). “Permafrost Hydrology”. *Springer Science & Business Media*.

World Economic Forum. (2019). *The Global Risks Report 2019* https://www.weforum.org/reports/the-global-risks-report-2019 (Accessed 15 September 2020)

Zhang, T., Barry, R. G., Knowles, K., Heginbottom, J. A., and Brown, J. (1999). “Statistics and characteristics of permafrost and ground-ice distribution in the Northern Hemisphere”. *Polar Geography*, 23(2), 132–154.

Appendix A: Statistical Results

IV	DV	Observations	Model	R^2 /psuedo R^2	Model P-Value	DV Coefficient	Coefficient P-Vlaue	Assumptions not met
Total Hazard	Condition Score	139	OLS	0.026	0.0565	-0.0125	0.057	Errors Normally Distributed
Total Hazard	Log(Condition Score)	139	OLS	0.018	0.118	-0.00008	0.118	Errors Normally Distributed
Total Hazard	Sqrt(Condition Score)	139	OLS	0.022	0.079	-0.0008	0.079	Errors Normally Distributed
Total Hazard	Condition Score	133	OLS	0.035	0.032	-0.042	0.032	Errors Normally Distributed
Total Hazard	Log(Condition Score)	133	OLS	0.028	0.053	-0.0003	0.053	Errors Normally Distributed
Total Hazard	Sqrt(Condition Score)	133	OLS	0.032	0.039	-0.0026	0.039	Errors Normally Distributed
Total Hazard	Condition Score	125	OLS	0.046	0.016	-0.045	0.016	Errors Normally Distributed/Independent
Total Hazard	Log(Condition Score)	125	OLS	0.05	0.012	-0.0003	0.012	Errors Independent
Total Hazard	Sqrt(Condition Score)	125	OLS	0.048	0.014	-0.0029	0.014	Errors Independent
Hazard/Area	Condition Score	139	OLS	0.022	0.079	-3.13	0.08	Errors Normally Distributed
Hazard/Area	Log(Condition Score)	139	OLS	0.014	0.168	-0.019	0.168	Errors Normally Distributed
Hazard/Area	Sqrt(Condition Score)	139	OLS	0.018	0.111	-0.188	0.111	Errors Normally Distributed
Hazard/Area	Condition Score	133	OLS	0.002	0.629	2.93	0.629	Errors Normally Distributed
Hazard/Area	Log(Condition Score)	133	OLS	0.003	0.507	0.0317	0.507	Errors Normally Distributed
Hazard/Area	Sqrt(Condition Score)	133	OLS	0.003	0.56	0.234	0.56	Errors Normally Distributed
Hazard/Area	Condition Score	125	OLS	0	0.898	0.98	0.898	Errors Normally Distributed/Independent
Hazard/Area	Log(Condition Score)	125	OLS	0.001	0.716	0.0189	0.716	Errors Independent
Hazard/Area	Sqrt(Condition Score)	125	OLS	0	0.81	0.116	0.81	Errors Independent
Total Hazard	Condition Score/100	139	Logistic	-0.7117	N/A	0.001	0.248	None
Hazard/Area	Condition Score/100	139	Logistic	-0.608	N/A	0.308	0.009	None

Appendix B: Facility Data

Building Number	Year Built	MDI	BCI	A10	Baseline	Weighted AVG
97	1959	80	58	86	90	81
98	1959	80	65	86	90	83
99	1959	60	78	85	50	66
100	1959	48	81	-	75	77
101	2015	80	98	94	95	95
102	2013	80	90	91	85	88
103	2006	60	88	93	95	93
104	1952	60	89	86	85	86
105	1959	80	40	86	90	76
106	1952	72	74	85	50	65
107	1959	80	81	66	25	49
112	1956	92	83	-	25	44
114	1952	72	88	85	75	81
115	1952	72	66	86	40	58
116	1952	72	70	85	70	74
117	1952	72	71	85	70	74
118	2004	80	86	-	60	69
121	1952	2		-	70	70
122	1952	72	88	85	80	83
123	1952	60	88	85	75	81
124	1952	72	88	85	80	83
125	1952	72	86	85	85	85
126	1952	72	84	85	85	85
127	1952	72	76	85	60	70
131	1952	72	86	85	80	83
132	1952	72	88	85	75	81
133	1952	72	91	85	75	81
134	1952	72	68	86	50	64
135	1952	72	77	85	75	78
142	1952	72	86	85	75	80
143	1952	72	66	86	50	63
144	1952	72	71	85	25	52
145	1952	72	68	86	50	63
151	1952	72	76	85	50	65
200	1988	80	84	-	25	45
201	1952	28	6	-	75	52
203	1952	72	89	85	90	88
205	1952	72	88	85	90	88

206	1952	72	91	85	90	89
211	1952	48	83	-	75	78
212	1952	72	66	86	25	50
214	1952	5	86	-	25	45
215	1952	72	75	85	50	65
216	1952	72	89	85	50	68
231	1952	72	67	85	75	75
233	1952	72	71	85	60	69
236	1955	20	68	41	25	40
241	1953	71	83	-	40	54
243	1952	72	49	85	30	48
245	1952	72	91	85	40	64
246	1952	72	73	85	40	59
251	1952	33	9	-	25	20
252	1952	72	56	-	85	75
253	1952	72	84	85	50	67
254	1952	72	67	85	40	58
255	1952	72	82	85	40	62
256	1952	72	66	86	40	58
274	1953	60	82	-	50	61
287	1955	80	80	-	50	60
321	1953	72	59	85	40	56
322	1953	72	78	85	60	71
323	1953	72	74	85	50	65
324	1953	72	51	85	50	59
325	1952	72	77	85	75	78
331	1953	72	64	85	50	62
333	1952	72	53	85	50	60
334	1952	72	52	85	50	59
335	1953	72	73	85	50	64
336	1953	72	68	85	50	63
341	1953	72	32	-	50	44
342	1953	72	64	85	25	50
343	1953	72	60	76	25	46
344	1953	72	61	76	50	59
345	1952	72	68	74	75	73
346	1953	60	5	-	75	52
351	1953	72	57	76	75	71
352	1952	72	69	76	75	74
353	1953	72	64	76	40	55
354	1953	72	66	76	50	60

355	1953	28	84	-	50	61
356	1953	72	52	76	75	69
360	1982	25	-	-	50	50
361	2008	72	75	-	95	88
362	1953	20	79	69	50	62
366	1953	48	82	-	-	82
367	1953	20	30	-	75	60
445	1953	60	25	-	25	25
461	1953	28	62	78	50	60
551	1953	33	30	-	25	27
553	1953	49	25	-	25	25
555	1953	48	84	25	50	52
561	1952	75	84	-	50	61
562	1953	28	81	-	-	81
563	1953	33	30	-	50	43
564	1953	28	82	-	-	82
566	1953	24	-	-	50	50
570	1953	24	-	-	25	25
571	1953	33	-	-	50	50
577	1952	28	86	-		86
604	1955	81	71	-	50	57
605	1953	68	77	35	50	53
606	1953	80	56	33	25	35
608	1953	64	74	72	50	62
610	1953	61	49	37	50	46
619	1952	52	80	-	50	60
622	1990	68	88	-	75	79
623	1952	80	82	-	25	44
624	1952	80	59	-	50	53
625	1987	68	86	-	75	79
628	1953	24	80	-	50	60
629	1953	80	79	-	-	79
630	1955	80	66	-	50	55
703	1953	72	54	76	50	57
705	1953	72	65	76	50	60
707	1953	72	60	76	50	59
780	1988	20	-	-	50	50
801	1958	60	86	-	50	62
807	2005	24	-	-	95	95
836	1958	67	-	-	50	50
933	1959	24	81	-	50	60

935	1956	48	82	-	50	61
937	2009	24	-	-	95	95
972	1953	24	42	-	50	47
974	1953	24	42	-	50	47
977	1973	48	-	-	75	75
992	1955	48	81	-	95	90
994	2012	71	-	-	95	95
996	1974	39	64	-	90	81
997	2012	71	-	-	95	95
1090	1952	24	-	-	75	75
1091	1952	24	-	-	80	80
1201	1952	20	85	-	80	82
1307	1953	88	79	-	80	80
1308	1969	33	88	-	90	89
1309	1995	68	92	-	95	94
1391	1987	99	75	-	50	58
1393	2010	71	-	-	95	95
1401	1953	99	84	-	50	61
1408	1955	48	82	-	50	61
1409	1956	53	85	-	50	62
1410	1956	33	73	-	50	58
1411	1956	60	71	-	80	77
1824	1954	99	79	-	75	76
1832	1974	52	82	-	50	61
1891	2014	99	80	-	-	80
1971	1952	14	83	-	50	61
1972	2010	84	78	-	-	78
1975	1952	84	82	-	50	61
2012	1953	-	54	-	-	54
2403	1956	61	79	-	50	60
2405	1956	71	12	-	-	12
4002	1960	99	80	60	50	60
4003	1960	90	70	-	50	50
4008	2002	99	81	-	75	77
4013	1959	67	70	-	75	75
4016	1960	80	80	60	25	47
7702	1992	-	82	-	95	91

MDI: Mission Dependency Index
BCI: Building Condition Index
A10: Foundation Assessment Score

Appendix C: ArcMap Instructions

Part 1: Data Import and Transformation

1. Open ArcMap and drag the aerial photography and digital elevation model files into the table of contents.
2. Check that each layer is in the same coordinate system and transform if necessary. By right clicking the layer, choosing the layer properties option and locating the coordinate system tab, transformations can be completed.

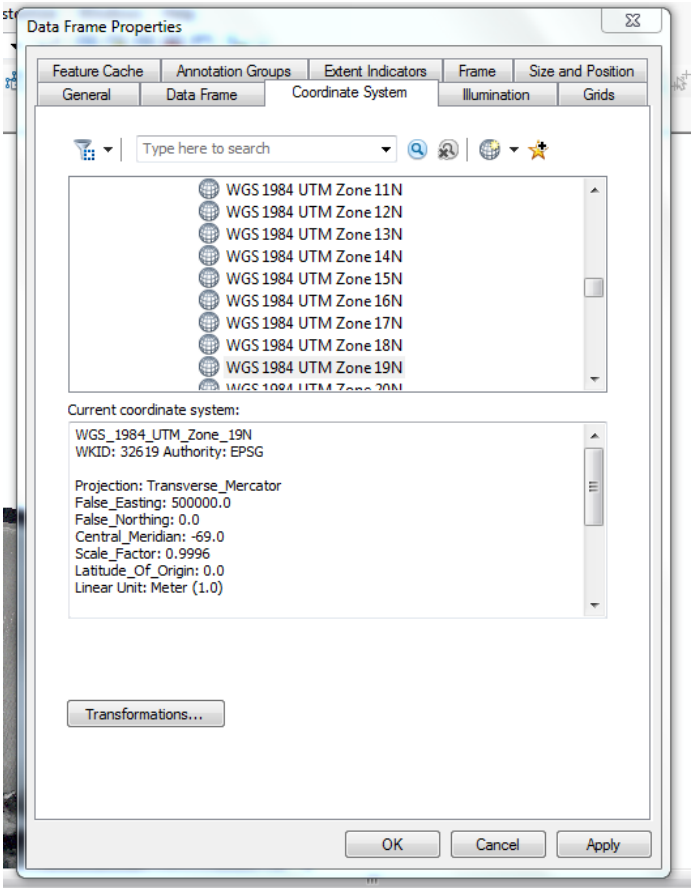

3. If data is not geocoded, it must be georeferenced in order to use in analysis. Bring the ArcMap Georeferencing toolkit into view by selecting the customize tab in the main screen and hovering over the toolkit option, select georeferencing.

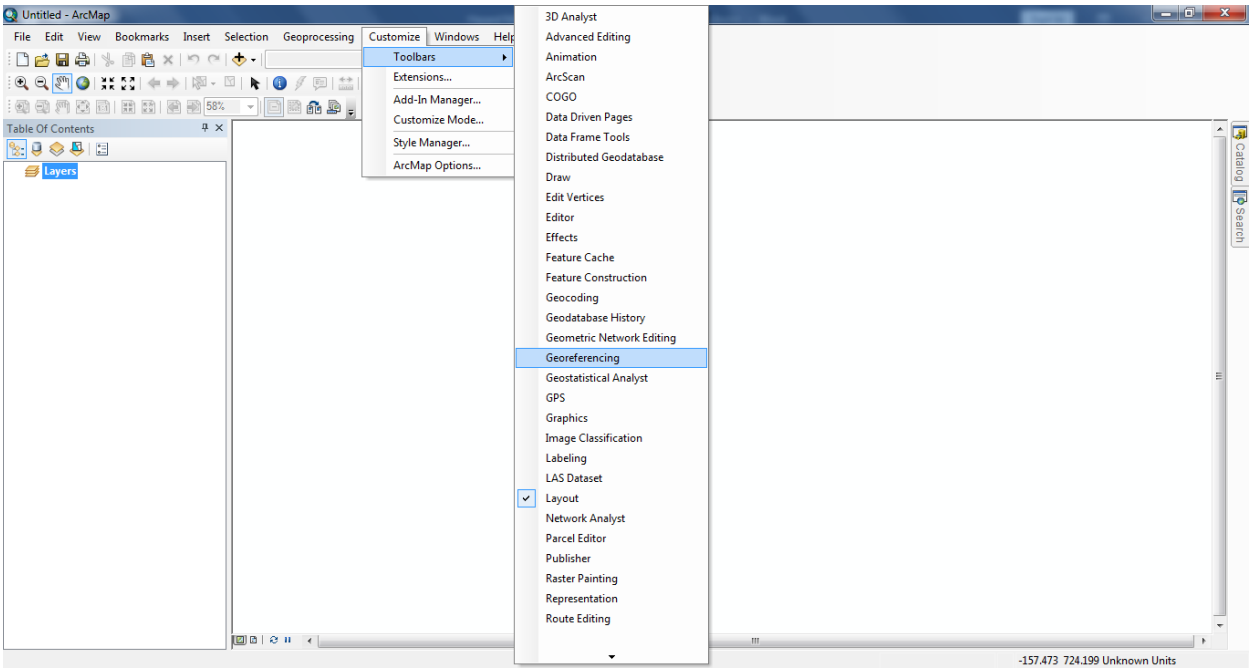

4. In the file dropdown next to Georeferencing, choose the file of interest. On the georeferencing tab, select fit to display in a view that will allow for side by side comparison, then zoom out to compare. Next choose the first icon and add control points first on the unreferenced photo then on the referenced layer. Once aligned, click update georeferencing in the georeferencing tab to save.

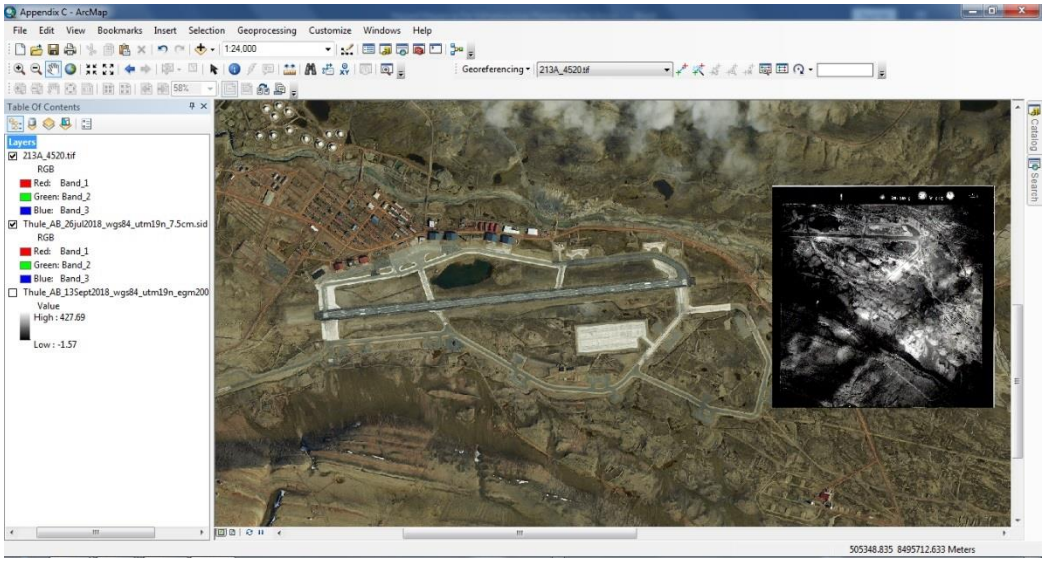

Part 2: Data Analysis

1. The first step to visual analysis of the data is to organize the outputs. Using the catalog tab, create a new file geodatabase in an accessible folder in the new tab. Within this geodatabase create a new feature dataset named visible features. Within this dataset create a new feature class for each feature that is identified. Once this system is created, the features will appear in the table of contents. By right clicking and starting to edit them, the create features window will appear. Click on each feature and select the construction tool at the bottom. Auto-complete Freehand is the most useful for freehand identification.

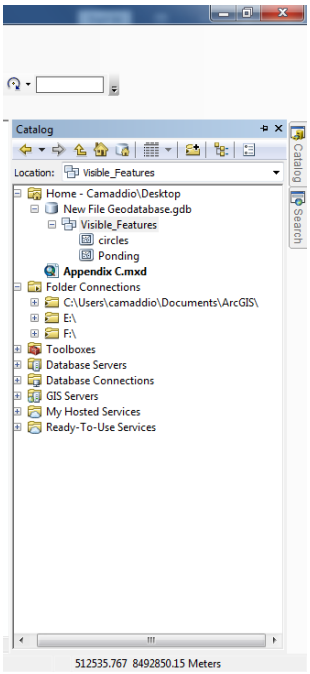

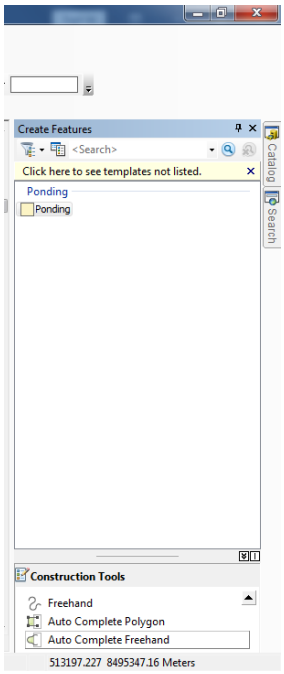

2. After each feature is identified, right click on its name in the table of contents and open the attribute table. In the shape column, right click, and using the calculator, input the hazard score it will be assigned. Once this is complete for each feature, convert each feature to a raster using the shape (now the hazard) as the field. Each feature now has its own raster that can be used separately or combined using the mosaic tools.

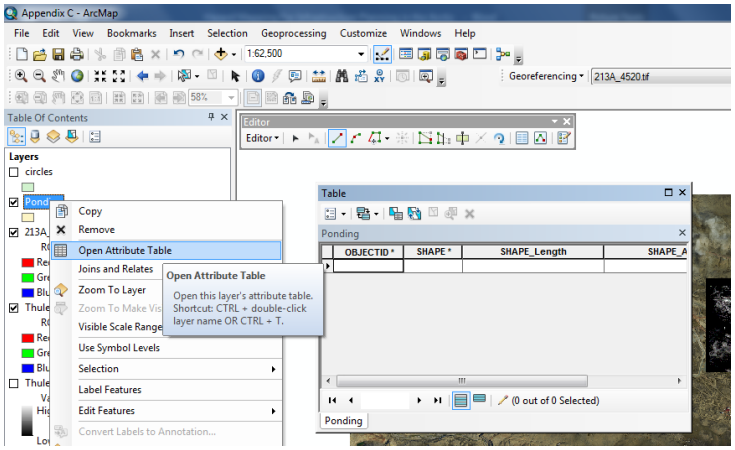

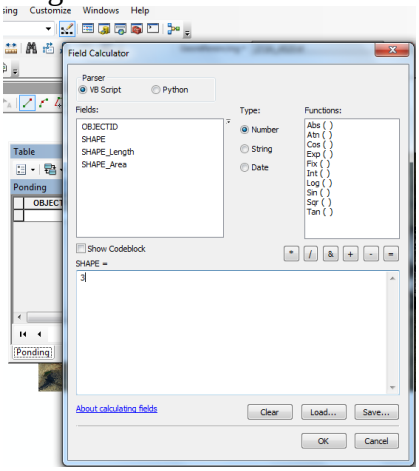

3. The accumulation hazard is created using the digital elevation model and hydrology toolkit. An overview of this toolkit is located at:
   https://desktop.arcgis.com/en/arcmap/10.3/tools/spatial-analyst-toolbox/an-overview-of-the-hydrology-tools.htm
   The goal of this analysis is to visualize the major drainage pathways and assign them a hazard score. The flow accumulation tool ultimately provides the data needed to assign the hazard. This tool creates a raster with the cell value indicating the number of cells that accumulate into it. Using the reclassification tool, ranges of accumulation values can be assigned hazard scores. This process takes trial and error to visualize the paths of acculturation in three distinct levels.

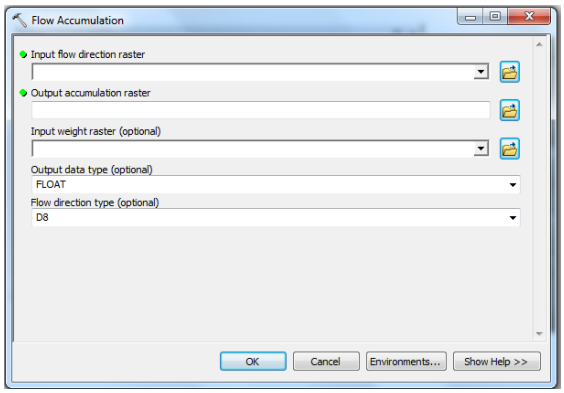

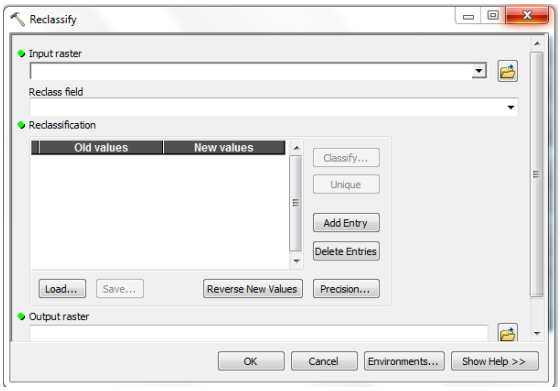

4. The final analysis tool used is the slope tool. It is located in the spatial analyst tool kit, under the surface category, or by searching slope in the search bar. This tool takes an input of a digital elevation model and outputs the slope in angle or percent as a raster. Hazard scores are again assigned using the reclassification tool.
5. Each of the three hazards can be visualized separately by checking and unchecking the layer visibility on the left of the table of contents. The visual representation of each hazard can be chosen by right clicking the layer, choosing properties at the bottom and selecting the symbology tab.

Part 3: Cumulative hazard calculation and spatial join

1. Use the cell statistics tool to combine the three hazards into one value. The raster calculator tool cannot be used if the extents of the raster's are different, which they are in this case. The cell statistics tool takes each raster's cell values and output the desired statistic for the new raster. Once this is complete, use the raster to points tool to convert these values into points. Choose the number of points based on time available for commutation and processor power.

2. Next, the building footprints are imported as shapefiles from the available data. Right click on this layer and choose the join and relates item from the dropdown and choose the join option. To add the foundation assessment score, choose the join attributes from a table and select the building number for both fields.

3. The last step is to join the foundation layer to the hazard points. Right click on the foundations layer, now selecting join based on spatial location. Select the first option to calculation values summarizing all the points that fall within each polygon.

REPORT DOCUMENTATION PAGE

Form Approved
OMB No. 0704-0188

1. REPORT DATE *(DD-MM-YYYY)*	2. REPORT TYPE	3. DATES COVERED *(From - To)*
25-03-2021	Graduate Research Paper	Aug 2020 - Mar 2021

4. TITLE AND SUBTITLE
Hazard Mapping for Infrastructure Planning in the Arctic

5a. CONTRACT NUMBER

5b. GRANT NUMBER

5c. PROGRAM ELEMENT NUMBER

6. AUTHOR(S)
Amaddio, Christopher I, 1st Lt

5d. PROJECT NUMBER

5e. TASK NUMBER

5f. WORK UNIT NUMBER

7. PERFORMING ORGANIZATION NAME(S) AND ADDRESS(ES)
Air Force Institute of Technology
Graduate School of Engineering and Management (AFIT/EN)
2950 Hobson Way
Wright-Patterson AFB OH 45433-7765

8. PERFORMING ORGANIZATION REPORT NUMBER
AFIT-ENV-MS-21-M-201

9. SPONSORING/MONITORING AGENCY NAME(S) AND ADDRESS(ES)
821st Support Squadron, Thule Air Base
Civil Engineer Flight Commander
PSC 1501 Box 1229
APO, AE 09704
DSN: (312) 629-3274

10. SPONSOR/MONITOR'S ACRONYM(S)
N/A

11. SPONSOR/MONITOR'S REPORT NUMBER(S)

12. DISTRIBUTION/AVAILABILITY STATEMENT
Distribution Statement A. Approved for Public Release;Distribution Unlimited

13. SUPPLEMENTARY NOTES

14. ABSTRACT
Using modern high-resolution aerial photographs, LiDAR, historical aerial photographs, and facility data, a hazard mapping effort identified risks to infrastructure at Thule Air Base, Greenland, based on visible terrain features, surface hydrology, and slope; the distribution of these risks were then compared to existing foundation damage. The analysis indicated abundant and widespread geotechnical hazards at Thule Air Base and a weak relationship to existing foundation damage that requires more research to understand. The resulting hazard maps provide a critical tool for risk assessment and planning as well as a model for other locations to follow.

15. SUBJECT TERMS
Arctic, Hazards, GIS, Permafrost, Infrastructure

16. SECURITY CLASSIFICATION OF:			17. LIMITATION OF ABSTRACT	18. NUMBER OF PAGES	19a. NAME OF RESPONSIBLE PERSON
a. REPORT	b. ABSTRACT	c. THIS PAGE			Dr. Alfred E. Thal, AFIT/ENV
					19b. TELEPHONE NUMBER *(Include area code)*
U	U	U	UU	113	312-785-3636 x7401 Alfred.thal@afit.edu